Biological applications of localised surface plasmonic phenomenae

D.A. Stuart, A.J. Haes, C.R. Yonzon, E.M. Hicks and R.P. Van Duyne

Abstract: Researchers and industrialists have taken advantage of the unusual optical, magnetic, electronic, catalytic, and mechanical properties of nanomaterials. Nanoparticles and nanoscale materials have proven to be useful for biological uses. Nanoscale materials hold a particular interest to those in the biological sciences because they are on the same size scale as biological macromolecules, proteins and nucleic acids. The interactions between biomolecules and nanomaterials have formed the basis for a number of applications including detection, biosensing, cellular and *in situ* hybridisation labelling, cell tagging and sorting, point-of-care diagnostics, kinetic and binding studies, imaging enhancers, and even as potential therapeutic agents. Noble metal nanoparticles are especially interesting because of their unusual optical properties which arise from their ability to support surface plasmons. In this review the authors focus on biological applications and technologies that utilise two types of related plasmonic phenomonae: localised surface plasmon resonance (LSPR) spectroscopy and surface-enhanced Raman spectroscopy (SERS). The background necessary to understand the application of LSPR and SERS to biological problems is presented and illustrative examples of resonant Rayleigh scattering, refractive index sensing, and SERS-based detection and labelling are discussed.

1 Introduction

The intense scattering and absorption of light from noble metal nanoparticles is the source of some of the beautiful colours in stained glass windows and has attracted the interest of scientists for generations. These nanoparticles exhibit a strong UV-vis absorption band that is not present in the spectrum of the bulk metal [1–8]. Although scientists have learned that the characteristic hues of these noble metal nanoparticle suspensions arise from their strong interaction with light, the advent of the field of nanoparticle optics has allowed for a deeper understanding of the relationship between material properties such as composition, size, shape, and local dielectric environment and the observed colour of a metal suspension. An understanding of the optical properties of noble metal nanoparticles holds both fundamental and practical significance. Fundamentally, it is important to systematically explore the nanoscale structural and local environmental factors that cause optical property variation, as well as provide access to regimes of predictable behaviour. Practically, the tunable optical properties of nanostructures can be applied as materials for surface-enhanced spectroscopy [9–13], optical filters [14, 15], plasmonic devices [16–19] and sensors [20–34].

One of the most interesting properties of noble metal nanoparticles arises from their ability to support a localised surface plasmon resonance (LSPR). The LSPR results when the incident photon frequency is resonant with the collective oscillation of the conduction electrons of the nanoparticle. The simplest theoretical approach available for modelling the optical properties of nanoparticles is the Mie theory estimation of the extinction of a metallic sphere in the long wavelength, electrostatic dipole limit. In the following equation [35]:

$$E(\lambda) = \frac{24\pi N_A a^3 \varepsilon_m^{3/2}}{\lambda \ln(10)} \left[\frac{\varepsilon_i}{(\varepsilon_r + 2\varepsilon_m)^2 + \varepsilon_i^2} \right] \quad (1)$$

$E(\lambda)$ is the extinction which is, in turn, equal to the sum of absorption and Rayleigh scattering, N_A is the areal density of nanoparticles, a is the radius of the metallic nanosphere, ε_m is the dielectric constant of the medium surrounding the metallic nanosphere (assumed to be a positive, real number and wavelength independent), λ is the wavelength of the absorbing radiation, ε_i is the imaginary portion of the metallic nanosphere's dielectric function, and ε_r is the real portion of the metallic nanosphere's dielectric function. The LSPR condition is met when the resonance term in the denominator ($(\varepsilon_r + 2\varepsilon_m)^2$) approaches zero. Even in this most primitive model, it is abundantly clear that the LSPR spectrum of an isolated metallic nanosphere embedded in an external dielectric medium will depend on the nanoparticle radius a, the nanoparticle material (ε_i and ε_r), and the nanoenvironment's dielectric constant (ε_m). Furthermore, when the nanoparticles are not spherical, as is always the case in real samples, the extinction spectrum will depend on the nanoparticle's in-plane diameter, out-of-plane height, and shape. In this case the resonance term from the denominator of (1) is replaced with:

$$(\varepsilon_r + \chi\varepsilon_m)^2 \quad (2)$$

where χ, a shape factor term [11] is a term that describes the nanoparticle's aspect ratio. The values for χ increase from two (for a sphere) up to, and beyond, values of 17 for a 5:1 aspect ratio nanoparticle. In addition, many of the samples

© IEE, 2005

IEE Proceedings online no. 20045012
doi:10.1049/ip-nbt:20045012
Paper first received 22nd December 2004

The authors are with the Department of Chemistry, Northwestern University, 2145 Sheridan Road, Evanston, IL 60208-3113, USA

E-mail: vanduyne@chem.northwestern.edu

considered in this work contain an ensemble of nanoparticles that are supported on a substrate. Thus, the LSPR will also depend on interparticle spacing and the substrate dielectric constant.

LSPR excitation results in wavelength selective absorption with extremely large molar extinction coefficients $\sim 3 \times 10^{11}$ 1/M cm [36], resonant Rayleigh scattering [37, 38] with an efficiency equivalent to that of 10^6 fluorophors [39] and the enhanced local electromagnetic fields near the surface of the nanoparticle which are responsible for the intense signals observed in all surface-enhanced spectroscopies, e.g. surface-enhanced Raman scattering (SERS) and surface-enhanced fluorescence [11, 26, 27].

2 Synthetic methods to produce nanoparticles

One of the aims of any application, particularly for sensing research, is to be able to generate reproducible results. In nanobiological applications, this translates directly into a critical need to understand and control the synthetic methods used to generate novel nanoscale materials. At the nanoscale, there are many options available ranging from nanoparticles in solution, to surface-bound nanoparticles, to nanoparticles entrapped in a three-dimensional matrix. With this plethora of potentially useful nanomaterial classes, there exist a large number of fabrication methods to controllably and reproducibly produce these samples. In this Section, we will discuss the most pertinent synthetic methods used in biosensing application: chemical synthesis and lithographic techniques.

2.1 Nanoparticle synthesis by chemical reduction

The synthesis of inorganic nanocrystals with controllable shapes and sizes has been a driving force in much of materials research. This has been characterised by rapid progress in the past few years with synthesis of spheres [40, 41], rods [42–44], triangular prisms [45–47], disks [48–50], cubes [51] and branched nanocrystals [52]. These structures are compelling for their use in biolabelling and biosensing. In this review, we will concentrate on the synthesis and use of noble metal nanoparticles for biological sensing platforms. The most commonly prepared shapes are spheroids, triangular prisms, rods and cubes (Fig. 1). All of these shapes are based on the reduction of a metal salt to produce nanoparticles with varied shapes and sizes. A different but related synthetic technique is the electrochemical reduction of metal salts in the presence of a surfactant or template [53–57]. These methods are most effective at producing large aspect ratio particles. The effect of nanoparticle shape on the optical properties is clearly illustrated in Fig. 2, which shows the scattering spectra from four different morphologies [58].

2.2 Core-shell morphologies

Core-shell particles encompass a range of sample types from metal surrounding metal [59, 60] to dielectric surrounding metal. Most notably is the work of Ung *et al.* [61]. These particles are produced by first creating the metal cores by one of the standard reduction reactions described above. To stabilise the colloids and remove the citrate ions, the colloids are mixed and allowed to react with an aminoalkane or thioalkane. Once the citrate has been completely displaced, the colloidal solution is allowed to react with a solution of active silica to form the shell (Fig. 3*a*). After 24 h, the particles can be used for further chemical modification or to increase the shell thickness [61–63]. Transmission electron microscopy (TEM) and dark-field optical micrographs of

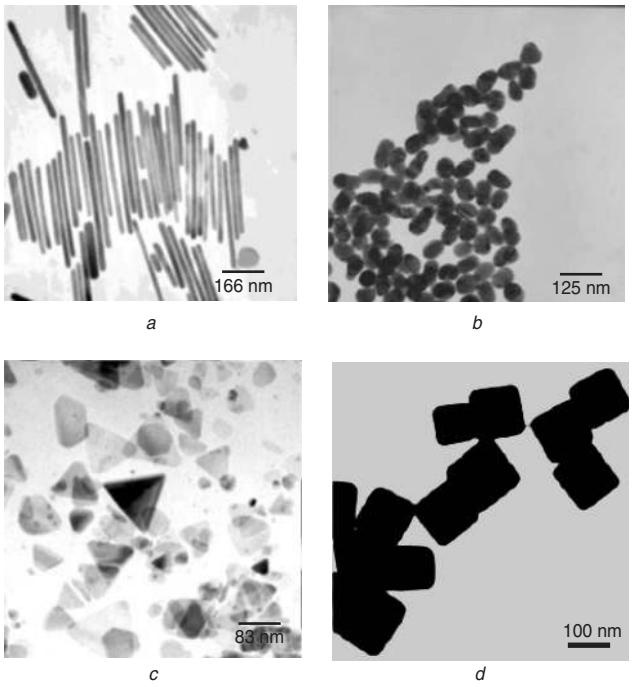

Fig. 1 *Bright field TEM images*
a Gold nanorods (sample provided by Catherine Murphy)
b Gold colloids
c Silver triangular prisms
d Silver nanocubes (Reproduced with permission from [51]. Copyright 2002)

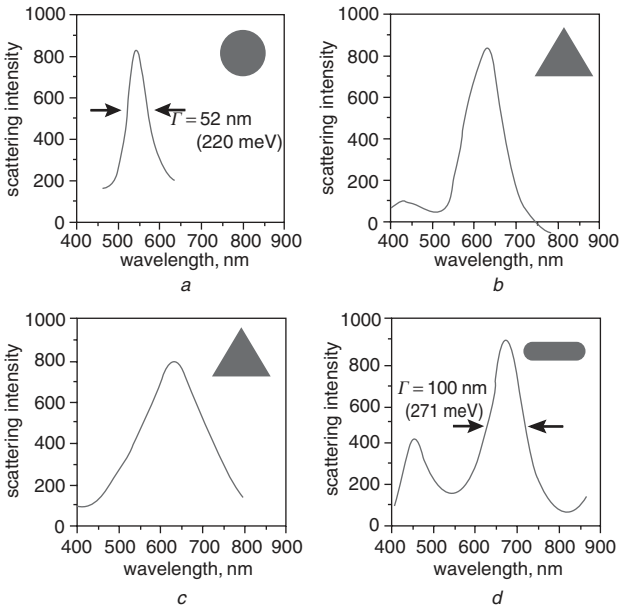

Fig. 2 *Resonant Rayleigh scattering spectra of four individual Ag nanoparticles*
a The single resonance near 540 nm signifies a spherical nanoparticle with a diameter near 50 nm
b and *c* The broad peaks near 650 nm with shoulders are indicative of platelet-shaped nanoparticles having a polygonal cross-section
d Two symmetric peaks, an intense one near 700 nm and weaker one near 450 nm, is suggestive of a rod-shaped nanoparticle that is approximately 40 nm in diameter and 300 nm long

this type of core-shell structure are shown in Fig. 3*b* and *c*. Recently, Yin *et al.* [64] have developed a simpler and faster method to silica coat particles. Their method involves suspension of aqueous phase particles within an isopropanol/water mixture followed by the direct addition of a small fraction of tetraethyl orthosilicate (TEOS). The TEOS

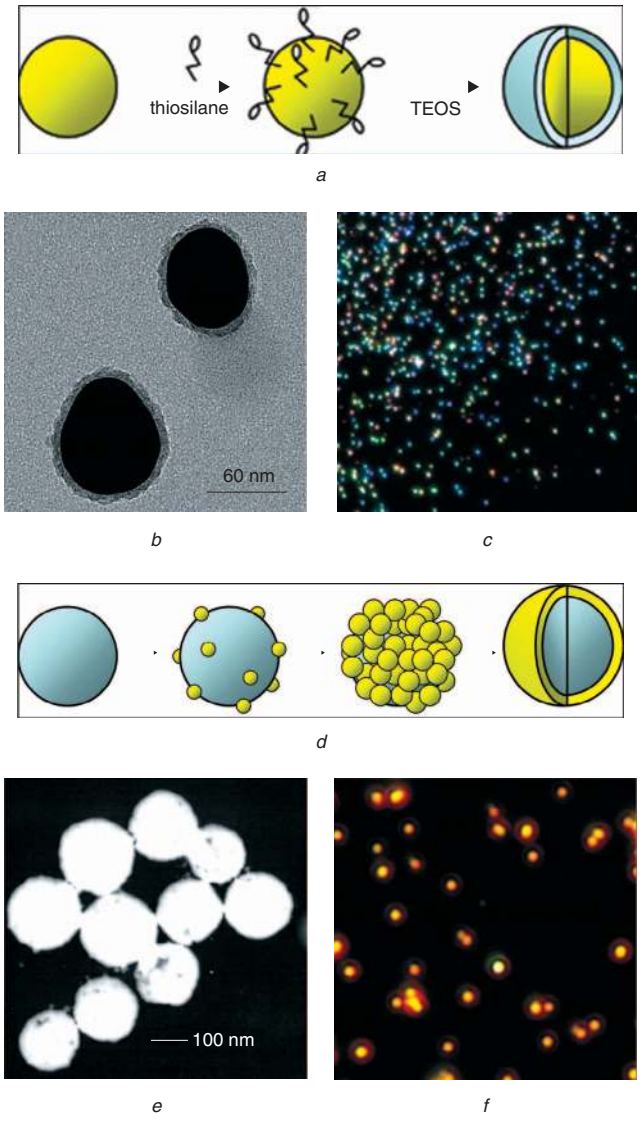

Fig. 3 *Schematic illustration and micrographs of core-shell nanoparticles*
a Metal nanoparticles are functionalized with mercapto-silanes, which serve as nucleation sites of the growth of the silica shell
b TEM micrograph of silica encapsulated metal nanoparticles
c Dark-field optical micrograph of the silica-encapsulated metal nanoparticles
d A dielectic core is decorated with small gold nanoparticles, which are then grown via electroless plating until a continuous shell is formed
e TEM micrograph of the dielectric core-metal shell nanoparticles
f Dark-field optical micrograph of the dielectric core-metal shell nanoparticles

quickly forms a silica shell around the nanoparticle indistinguishable from those created in the Ung *et al.* method. The Yin *et al.* method is rapid, but unsuitable for certain applications, notably the co-encapsulation of Raman-active species within the silica shell (see below), and the coating of particles formed in the presence of surfactants has met with limited success.

Another form of core-shell particles has a metal shell surrounding a dielectric centre. The dielectric core, usually silica, is produced by the Stöber method to produce monodispersed silica cores ranging in size from 80–500 nm [65, 66]. These particles are then functionalised with 3-aminopropyltrimethoxysilane. These functionalised particles are then reacted with small gold nanoparticles. The gold particles provide nucleation sites for the growth of the metallic shell from metal salts in solution. NH_4OH is added to produce preferential deposition onto the surface, rather than initiate new particle formation in solution (Fig. 3*d*) [65–69]. The TEM and dark-field optical micrographs of this type of nanoshell are shown in Figs. 3*e* and 3*f*.

2.3 Lithographic techniques

All nanoparticle fabrication methods discussed thus far are used to create suspensions of nanoparticles in solution. Another class of techniques addresses substrate-bound nanostructure fabrication. The standard approach for making substrate-bound nanostructures is electron beam lithography (EBL). In EBL, the desired pattern is serially produced by exposing a thin layer of photo-resist to high energy electrons, followed by chemical development and deposition of the noble metal, Fig. 4*a*. Several research groups have focused on the optical properties of two-dimensional arrays in order to utilise these nanoparticle assemblies as surface-enhanced spectroscopy substrates [70–72]. While EBL provides exquisite control over nanoscale morphology, it is an expensive and time-consuming technique. An alternative method for the large-scale production of surface-bound nanoparticle arrays is nanosphere lithography (NSL).

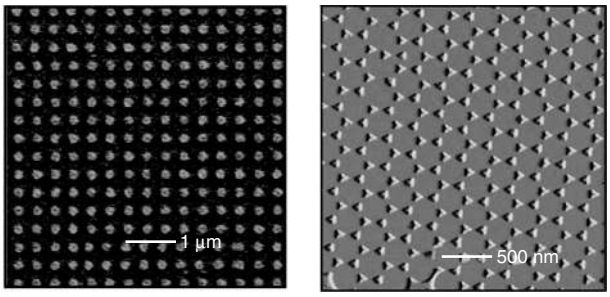

Fig. 4
a Scanning electron micrograph image of electron beam lithography arrays. Cylindrical nanoparticles with a diameter of 200 nm and heights of 40 nm Ag in square arrangement with a lattice spacing of 350 nm. Reproduced with permission from [13]. Copyright 2003, The American Chemical Society
b Atomic force microscopy micrograph of the nanosphere lithography arrays. Triangular nanoparticles with perpendicular bisectors of 100 nm and heights of 50 nm Ag

NSL is a powerful fabrication technique to inexpensively produce nanoparticle arrays with controlled shape, size, and interparticle spacing [73]. Every NSL structure begins with the self-assembly of size-monodispersed nanospheres of diameter D to form a two-dimensional colloidal crystal deposition mask [8, 73–75]. As the solvent evaporates, capillary forces draw the nanospheres together, and the nanospheres crystallise into a hexagonally close-packed pattern on the substrate. As in all naturally occurring crystals, nanosphere masks include a variety of defects that arise as a result of nanosphere polydispersity, site randomness, point defects, line defects, and polycrystalline domains. Typical defect-free domain sizes are in the 10–100 μm range. Following self-assembly of the nanosphere mask, a metal or other material is then deposited by thermal evaporation, electron beam deposition, or pulsed laser deposition, Fig. 4*b*. After metal deposition, the nanosphere mask is removed, leaving behind surface-confined nanoparticles with triangular footprints.

3 Sensing with noble metal nanostructures

It is apparent from (1) that the location of the extinction maximum of noble metal nanoparticles is highly dependent

on the dielectric properties of the surrounding environment and that wavelength shifts in the extinction maximum of nanoparticles can be used to detect molecule-induced changes surrounding the nanoparticle. As a result, there are at least four different nanoparticle-based sensing mechanisms that enable the transduction of macromolecular or chemical-binding events into optical signals based on changes in the LSPR extinction or scattering intensity shifts in LSPR λ_{max}, or both. These mechanisms are: (i) resonant Rayleigh scattering from nanoparticle labels in a manner analogous to fluorescent dye labels [38, 39, 76–82]; (ii) nanoparticle aggregation [83]; (iii) charge-transfer interactions at nanoparticle surfaces [35, 84–88]; and (iv) local refractive index changes [20, 23–25, 27, 28, 84, 89–93].

3.1 Solution-phase nanoparticle sensing

Solution-phase nanoparticle-based sensing is a simple, yet powerful detection modality. Because many molecules of interest, particularly biological molecules, are in the aqueous phase, it is desirable to have a sensitive and specific detection system that is homogenous with the phase of the target molecule, thereby decreasing the need for extended sample preparation. Aggregation-based detection has become a mainstay in the clinical community since the development of the latex agglutination test, (LAT) in 1956 [94]. In the LAT and similar tests, biomolecular-specific antibodies are conjugated to latex microspheres which, when mixed with a solution (e.g. blood or urine) containing the target antigen, cause the latex spheres to form visible aggregates. Whereas LATs are effective and quite rapid (15 min to 1 h), they are inherently insensitive, relying on high concentrations of analytes and on the human eye as a detector.

In contrast, for solution-phase LSPR-based sensing, signal transduction depends on the sensitivity of the surface plasmon to interparticle coupling. When multiple particles in solution that support a localised surface plasmon are in close proximity (i.e. interparticle spacings less than the nanoparticle diameter), they are able to interact electromagnetically through a dipole coupling mechanism. This broadens and red shifts the LSPR, and small clusters of particles possess LSPR properties similar to those of a larger single particle. Two methods of detection readily lend themselves to monitoring these changes in the position of the LSPR: (i) UV-visible (UV-vis) extinction (absorption plus scattering); and (ii) resonant Rayleigh scattering spectroscopy.

Several papers have been published on a gold nanoparticle-based UV-vis technique for the detection of DNA. This colourimetric detection method is based on the change in absorbance spectra (i.e. colour) as particles are brought together by the hybridisation of complementary DNA strands [95, 96]. The limits of detection (LOD) reported are in the range of tens of femtomoles of target oligonucleotide. These nanoparticle aggregation assays represent a 100-fold increase in sensitivity over conventional fluorescence-based assays [77]. Recently, gold nanoshells, that is, silica beads with a thin gold coating, have been used to detect antigens in whole blood [22]. In these studies, gold nanoshells were functionalised with a specific immunoglobulin. The nanoshells were designed so that they exhibit plasmon resonances in the near-infrared between the water absorption band and the absorption of hemoglobin. Upon addition of the nanoshells to whole blood that contains the appropriate antigen, the plasmon resonance broadens, the intensity decreases, and a slight red shift in the plasmon resonance occurs. This immunoassay, which occurs in less than 30 min, is capable of detecting picogram/millilitre quantities

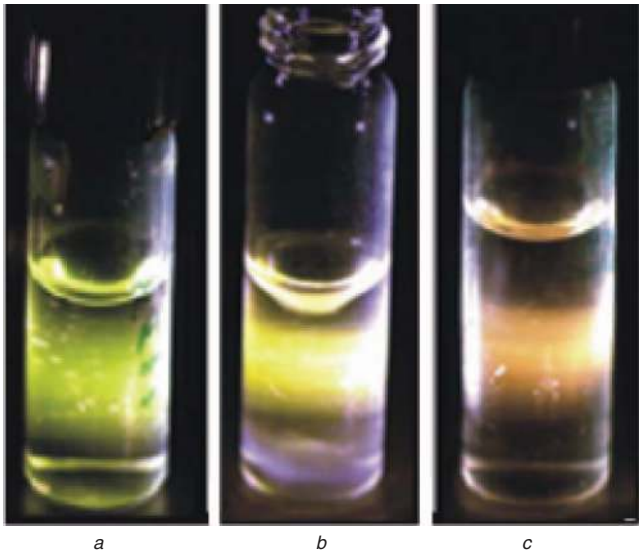

Fig. 5 *Time-lapse photographs of the rapid colourimetric test*
a 60 nm gold conjugates
b Stirring a 1:1 solution of IgG/gold conjugates and anti-human IgG/gold conjugates after approximately 3 min of stirring
c The same solution as (Fig. 5b), approximately 10 min later. Note the readily observed change in colour from green to orange, which is caused by interparticle coupling

of antigens. Sensing based on resonant Rayleigh scattering detection is a potentially more powerful, yet less well published, method than the colourimetric technique mentioned above [38, 97, 98]. Figure 5 demonstrates a simple sensing experiment, wherein the observed scattering colour changes as gold nanoparticles are drawn together by protein-protein interactions [99]. The disadvantages of this type of experiment is that the aggregation of the particles, necessary to induce interparticle coupling and generate a signal, is often irreversible, difficult to quantitate, and can lead to sufficient aggregation of the nanoparticles that they settle out of solution.

3.2 Nanoparticle labelling

Whereas the application of noble metal nanostructures as optical data storage elements is still under development, companies have already been formed to exploit noble metal nanostructures as biological labels. Nanoscale cylinders with stripes of different metals have been used as immunoassay tags; readout mechanisms have been based on both the extinction [98] and reflectivity [100]. In another example, Siiman and Burshteyn [101] have applied thin coatings of Ag or Au to latex microspheres that then act as flow cytometry labels. The noble metal island films make it easy to identify different subpopulations of white blood cells without significantly changing the bead's flow characteristics. When the labelled strand of DNA is exposed to a complimentary single strand of DNA immobilised on a glass substrate, the Au nanoparticle is bound to the surface. A flatbed scanner can be used to identify DNA matches.

Noble metal nanoparticles can go beyond acting as labels; recent advances show that changes in nanoparticle optical properties can act as the signal transduction mechanism in chemosensing and biosensing events. Haes *et al.* [26] and Malinsky *et al.* [84] have exploited the extreme LSPR sensitivity of NSL-fabricated nanoparticles to changes in local refractive index in order to sense small molecules, amino acids, proteins, and antibodies. The LSPR shifts systematically to lower energies as the local dielectric constant increases; accordingly, chemisorption of alkanethiols of increasing length cause a systematic red-shift

in the LSPR (3 nm/methylene unit) [84]. These nanoparticle sensors take advantage of tunable noble metal nanostructure optical properties in order to sensitively and selectively detect trace levels of the target molecule. These experiments are further detailed below.

3.3 Sensing on surfaces

A possible method for circumventing the difficulty of irreversible aggregate formation is to synthesise nanoparticles bound to substrates. Using this method, gold or silver nanoparticles can be chemically attached in a random fashion to a transparent substrate to detect proteins [32, 89]. In this format, signal transduction depends on changes in the nanoparticles' dielectric environment induced by solvent or target molecules (not via nanoparticle coupling). Using this chip-based approach, a solvent refractive index sensitivity of 76.4 nm/RIU has been found and a detection of 16 nM streptavidin can be detected [32, 89]. This approach has many advantages including: (i) a simple fabrication technique that can be performed in most labs; (ii) real-time biomolecule detection using UV-vis spectroscopy; and (iii) a chip-based design that allows for multiplexed analysis.

3.4 Sensing with nanoparticle arrays

The development of biosensors for the diagnosis and monitoring of diseases, drug discovery, proteomics, and the environmental detection of biological agents is an extremely significant problem [102]. Fundamentally, a biosensor is derived from the coupling of a ligand-receptor binding reaction [103] to a signal transducer. Much biosensor research has been devoted to the evaluation of the relative merits of various signal transduction methods including optical [104, 105], radioactive [106, 107], electrochemical [108, 109], piezoelectric [110, 111] magnetic [112, 113], micromechanical [114, 115] and mass spectrometric [116, 117]. The development of large-scale biosensor arrays composed of highly miniaturised signal transducer elements that enable the real-time, parallel monitoring of multiple species is an important driving force in biosensor research. Recently, several research groups have begun to explore alternative strategies for the development of optical biosensors and chemosensors based on the extraordinary optical properties of noble metal nanoparticles. Recently, it was demonstrated that nanoscale chemosensors and biosensors can be realised through shifts in the LSPR λ_{max} of triangular silver nanoparticles. These wavelength shifts are caused by adsorbate-induced local refractive index changes in competition with charge-transfer interactions at the nanoparticle surface. In this review, a detailed study is presented demonstrating that triangular silver nanoparticles fabricated by NSL function as extremely sensitive and selective nanoscale affinity chemosensors and biosensors. It will be shown that these nanoscale biosensors based on LSPR spectroscopy operate in a manner totally analogous to propagating surface plasmon resonance (SPR) sensors by transducing small changes in refractive index near the noble metal surface into a measurable wavelength shift response.

3.5 SPR sensors and their relationship to LSPR sensors

The potential of propagating SPR biosensors was recognised in early 1980s by Liedberg *et al.* [118], who were able to detect immunoglobulin antibodies by observing the change in critical angle when the antibodies bind selectively on a Au film. Propagating surface plasmons are evanescent electromagnetic waves that travel along the flat smooth metal-dielectric interfaces and arise from oscillations of the conduction electrons in the metal [119]. SPR sensors detect the local refractive index changes that occur when the target analyte binds to the metal film or nanoparticles. Surface refractive index sensors have an inherent advantage over optical biosensors that require a chromophoric group or other label to transduce the binding event, as in the labelling experiments described above.

It was realised that the sensor transduction mechanism of this LSPR-based nanosensor is analogous to that of SPR sensors (Table 1). Since their original discovery, SPR changes have been used in refractive-index-based sensing to detect analyte binding at or near a metal surface and has been widely used to monitor a broad range of analyte-surface binding interactions including the adsorption of small molecules [120–122], ligand-receptor binding [123–126], protein adsorption on self-assembled monolayers [127–129], antibody-antigen binding [130], DNA and RNA hybridisation [131–134] and protein-DNA interactions [135].

Important differences to appreciate between the SPR and LSPR sensors are the comparative refractive index sensitivities and the characteristic electromagnetic field decay lengths. SPR sensors exhibit large refractive index sensitivities ($\sim 2 \times 10^6$ nm/RIU) [120]. For this reason, the SPR response is often reported as a change in refractive index units. The LSPR nanosensor, on the other hand, has a modest refractive index sensitivity ($\sim 2 \times 10^2$ nm/RIU) [84]. Given that this number is four orders of magnitude smaller for the LSPR nanosensor in comparison to the SPR sensor, initial assumptions were made that the LSPR nanosensor would be 10 000 times less sensitive than the SPR sensor. This, however, is not the case. In fact, the two sensors are very competitive in their sensitivities. The short (and tunable) characteristic electromagnetic field decay length, l_d, provides the LSPR nanosensor with its enhanced sensitivity [26, 27]. These LSPR nanosensor results indicate that the decay length, l_d, is ~5–15 nm or ~1–3% of the light's wavelength and depends on the size, shape, and composition of the nanoparticles. This differs greatly from the 200–300 nm decay length or ~15–25% of the light's wavelength for the SPR sensor [120]. Also, the smallest footprint of the SPR and LSPR sensors differ. In practice, SPR sensors require at least a 10×10 μm area for sensing experiments. For LSPR sensing, this spot size can be minimised to a large number of individual sensing elements (1×10^{10} nanoparticles for a 2 mm spot size, nanosphere diameter = 400 nm) down to a single nanoparticle (with an in-plane width of ~20 nm) using single nanoparticle measurement techniques [81]. The nanoparticle approach can deliver the same information as the SPR sensor, thereby minimising its effective pixel size to the sub-100 nm regime. Because of the lower refractive index sensitivity, the LSPR nanosensor requires no temperature control whereas the SPR sensor (with a large refractive index sensitivity) requires temperature control. The final and most dramatic difference between the LSPR and SPR sensors is cost. Commercialised SPR instruments can vary between $150 000–$300 000, whereas the prototype and portable LSPR system costs less than $5000.

There is, however, a unifying relationship between these two seemingly different sensors. Both sensors' overall response can be described using the following equation [120]:

$$\Delta\lambda_{max} = m\Delta n(1-\exp(-2d/l_d)) \quad (3)$$

where $\Delta\lambda_{max}$ is the wavelength shift response, m is the refractive index sensitivity, Δn is the change in refractive index induced by an adsorbate, d is the effective adsorbate

Table 1: Comparison between SPR and LSPR sensors

Feature/characteristic	SPR	LSPR
Label-free detection	yes [122, 124, 131, 136]	yes [20, 28, 81, 84]
Distance dependence	~1000 nm [120]	~30 nm (size tunable) [26, 27]
Refractive index sensitivity	2×10^6 nm/RIU [105, 120, 121, 123]	2×10^2 nm/RIU [26, 84]
Modes	angle shift [137]	extinction [20]
	wavelength shift	scattering [81, 82]
	imaging	imaging [81, 82]
Requires temperature control	yes	no
Chemical identification	SPR-Raman	LSPR-SERS
Field portability	no	yes
Commercially available	yes	no
Cost	$150 000–$300 000	$5000 (multiple particles)
		$50 000 (single nanoparticle)
Spatial resolution	~10 × 10 μm [137, 138]	nanoparticle [81, 82, 97]
Nonspecific binding	minimal (determined by surface chemistry and rinsing) [105, 136, 137, 139, 140]	minimal (determined by surface chemistry and rinsing) [20]
Real-time detection	time scale = 10^{-1} – 10^3 s, planar diffusion [121, 122, 139, 141, 142]	time scale = 10^{-1} – 10^3 s, radial diffusion [81]
Multiplexed capabilities	yes [146, 147] [143, 144]	yes-possible
Small molecule sensitivity	good [121]	better [26]
Microfluidics compatibility	yes	possible

layer thickness, and l_d is the characteristic electromagnetic field decay length. It is important to note that for planar SPR sensors, this equation quantitatively predicts an adsorbate's effect on the sensor. When applied to the LSPR nanosensor, this exponential equation approximates the response for adsorbate layers but does provide a fully quantitative explanation of its response [26, 27]. Similar to the SPR sensor, the LSPR nanosensor's sensitivity was realised to arise from the distance dependence of the average induced square of the electric fields that extend from the nanoparticles' surfaces.

3.6 Real-time binding studies of SPR and LSPR sensors

To experimentally evaluate the relative performance of the two sensors, side by side comparisons were conducted. The exact procedures followed the standard experimental protocols established for the two sensing modalities [145].

For the SPR sensor, Au (50 nm) was evaporated onto glass coverslips with a thin Ti underlayer (10 nm). A BIACore 1000 (Neuchâtel, Switzerland) was used for all propagating SPR measurements reported. The mannose-functionalised substrate was incorporated into BIAcore cassettes by gluing the chip into the cassettes, and measurements were reported as changes in resonance angle ($\Delta\theta$), where $1^\circ = 10\,000$ RU. The LSPR sensors were fabricated using NSL to create Ag nanoparticle arrays (50 nm). LSPR extinction measurements were taken using a fibre optically-coupled spectrometer. All spectra in this study were from macroscopic measurements obtained in transmission mode using unpolarised white light. A home-built flow cell was used to control the surrounding environment of the Ag nanoparticles and the introduction of analytes [84].

The self-assembled monolayer (SAM) was prepared by immersing the coverslips in an ethanolic solution containing maleimide-terminated disulfide (1 mM) and 11-mercaptoundecyl tri(ethylene glycol) disulfide (EG3, 1 mM). After 12 h, the coverslips were rinsed with ethanol and dried under a stream of nitrogen. The substrates presenting maleimide-functional groups were immersed in methanolic solutions of 5 mM mannose thiol for 40 min, providing ~5% sugar-immobilised surfaces. The mannose-functionalised sensors were then exposed to 19 μM concanavalin A (Con A) in PBS buffer for 20 min (Fig. 6).

3.7 Real-time comparison of LSPR and SPR detection of Con A

To directly compare the sensing capabilities of SPR and LSPR sensors, the real-time response of Con A binding to a mannose-functionalised flat surface SPR sensor (Fig. 6*a*) and the LSPR Ag nanosensor (Fig. 6*b*) were investigated. Con A is a 104 kDa mannose-specific plant lectin comprised of a tetramer with dimensions of 6.32, 8.69, and 8.93 nm and has four binding sites [146]. The surface binding constant for Con A to a mannose-functionalised SAM was found to be 5.6×10^6 1/M by SPR imaging studies [147]. After the baseline SPR $\Delta\theta$ response of the mannose-functionalised Au surface in a running buffer environment was recorded, 19 μM Con A in buffer was injected. The sensor was then flushed with buffer to remove both non-specifically bound and Con A bound as the 1:1 mannose complex. Figure 6*a* illustrates the real-time monitoring of 19 μM Con A by the SPR $\Delta\theta$ shift. Similarly, the real-time LSPR response of Con A binding to the mannose-functionalised Ag nanonsensor was also probed. After the LSPR λ_{max} of the mannose-functionalised surface was recorded, 19 μM Con A was injected into the flow cell, then the sample was flushed with PBS buffer, and during this process the LSPR λ_{max} was measured in 5 s intervals for 20 min (Fig. 6*b*).

During the association phase, both the SPR and LSPR sensor showed a rapid response when Con A was exposed to the surface, which indicates strong Con A binding using two binding sites on the surface followed by weak 1:1 binding Con A binding as well as non-specific binding.

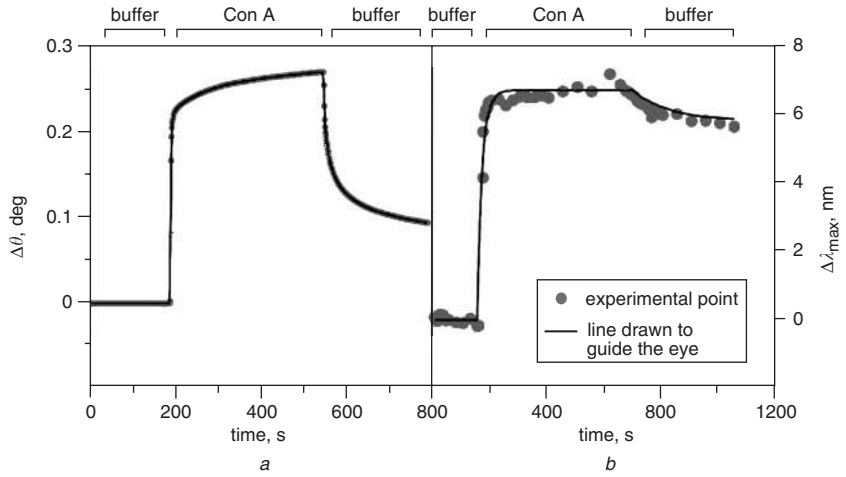

Fig. 6 *The real-time response of a sugar-functionalised sensor as 19 μM of Con A was injected in the cell following buffer injection*
a Mannose-functionalised SPR sensor
b Mannose-functionalised LSPR nanosensor

However, during the dissociation phase, when the Con A-bound SPR sensor surface was flushed with PBS buffer, the response decreased by 60% whereas the response decreased only by 14% for the LSPR sensor. It is hypothesised that this difference is the long-range decay length of the SPR sensor electromagnetic field ($l_d \approx 200$ nm) [120], compared to that of the LSPR sensor ($l_d \approx 5$–6 nm) [26, 27].

3.8 LSPR streptavidin and immunoglobulin sensing on nanoparticle arrays

As described above, nanoscale chemosensing and biosensing could be realised through shifts in the LSPR extinction maximum (λ_{max}) of these triangular silver nanoparticles [20, 23, 28, 84]. Signal transduction is an effect caused by shifts in wavelength produced by adsorbate-induced local refractive index changes in competition with charge-transfer interactions at the surfaces of nanoparticles. For these experiments, NSL was used to fabricate 25 and 50 nm Ag nanoparticles on glass or mica. The peak-to-peak wavelength shift noise of the baseline in repetitive experiments from this spectrometer is ~0.5 nm. Taking the limit of detection as three times this value, one can conservatively estimate the limit of detection of an assay will arise from a wavelength shift of 1.5 nm.

3.9 Streptavidin sensing using LSPR spectroscopy

The well-studied biotin-streptavidin system with its extremely high binding affinity ($K_a \sim 10^{13}$ 1/M) is chosen to illustrate the ultra-sensitive attributes of these LSPR-based nanoscale affinity biosensors. The biotin-streptavidin system has been studied in great detail by SPR spectroscopy and serves as an excellent model system for the LSPR nanosensor [20]. Streptavidin, a tetrameric protein, can bind up to four biotinylated molecules (i.e. antibodies, inhibitors, nucleic acids, etc.) with minimal impact on its biological activity and therefore will provide a ready pathway for extending the analyte accessibility of the LSPR nanobiosensor.

In the streptavidin detection scheme, the λ_{max} of the Ag nanoparticles were monitored during each surface functionalisation step (Fig. 7) [20]. First, the LSPR λ_{max} of the bare Ag nanoparticles was measured to be 561.4 nm (step A in Fig. 7). To ensure a well-ordered SAM on the Ag nanoparticles, the sample was incubated in a 3:1 Octanethiol : mercaptoundecanoic acid (OT/MUA) for 24 h. The LSPR λ_{max} (step B in Fig. 7) was measured to be

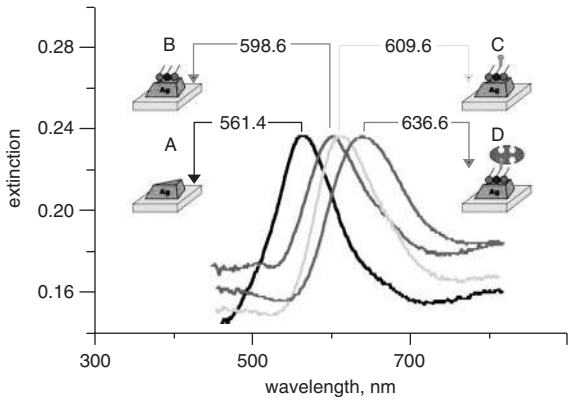

Fig. 7 *LSPR spectra of each step in the surface modification of NSL-derived Ag nanoparticles to form a biotinylated Ag nanobiosensor and the specific binding of streptavidin. Step A: Ag nanoparticles before chemical modification $\lambda_{max} = 561.4$ nm; Step B: Ag nanoparticles after modification with 1 mM 1:3 11-MUA: I-OT, $\lambda_{max} = 598.6$ nm; Step C: Ag nanoparticles after modification with 1 mM biotin $\lambda_{max} = 609.6$ nm. Step D: Ag nanoparticles after modification with 100 nm streptavidin $\lambda_{max} = 636.8$ nm. All extinction measurements were collected in a N_2 environment. (Reproduced with permission from [20]. Copyright 2002, The American Chemical Society)*

598.6 nm, a 38 nm red shift. Next, biotin was covalently attached via amide bond formation to carboxylated surface sites (step C in Fig. 7). The LSPR λ_{max} after biotin attachment (step C in Fig. 7) was measured to be 609.6 nm, corresponding to an additional +11 nm shift. Exposure to 100 nM streptavidin, resulted in LSPR $\lambda_{max} = 636.6$ nm (step D in Fig. 7) corresponding to an additional +27 nm shift.

3.10 Anti-biotin sensing using LSPR spectroscopy

A field of particular interest is the study of the interaction between antigens and antibodies. For these reasons we have chosen to focus the present LSPR nanobiosensor study on the prototypical immunoassay involving biotin and anti-biotin, an IgG antibody. Ag nanotriangles were synthesised using NSL to develop a LSPR biosensor that monitors the interaction between a biotinylated surface and free anti-biotin in solution [28]. The importance of this study is that it demonstrates the feasibility of LSPR biosensing with a biological couple whose binding affinity is significantly

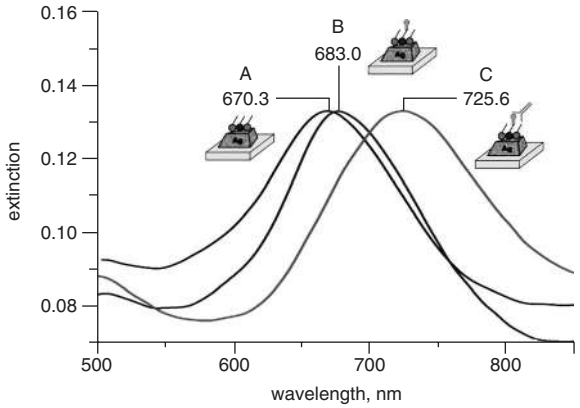

Fig. 8 *LSPR spectra for each step of the preparation of the Ag nanobiosensor, and the specific binding of anti-biotin to biotin. Step A: Ag nanoparticles after modification with 1 mM 3:1 1-OTl11-MUA, $\lambda_{max} = 670.3$ nm; Step B: Ag nanoparticles after modification with 1 mM biotin, $\lambda_{max} = 683.0$ nm; and Step C: Ag nanoparticles after modification with 700 nM anti-biotin, $\lambda_{max} = 725.6$ nm. All spectra were collected in a N_2 environment. Reproduced with permission from [28]. Copyright 2003, The American Chemical Society*

lower (1.9×10^6–4.98×10^8 1/M) than in the biotin/streptavidin model [20].

Each step of the functionalisation of the samples was monitored using UV-vis spectroscopy, as shown in Fig. 8 [28]. After a 24 h incubation in SAM, the LSPR extinction wavelength of the Ag nanoparticles was measured to be 670.3 nm (step A in Fig. 8). The LSPR wavelength shift due to biotin binding was measured to be +12.7 nm, resulting in a LSPR extinction wavelength of 683.0 nm (step B in Fig. 8). At this stage, the nanosensor was ready to detect the specific binding of anti-biotin. Incubation in 700 nM anti-biotin resulted in a LSPR wavelength shift of +42.6 nm, giving a λ_{max} of 725.6 nm (step C in Fig. 8).

3.11 Concentration-dependent response

It was revealed that if the analyte solution was decreased, the LSPR wavelength shift response also decreased. Subsequently, the full response of the sensor was determined over a wide concentration range. For this reason, variable analyte concentrations were exposed to a biotinylated LSPR chip to test the sensitivity of the system to different molecules. Specifically, the LSPR λ_{max} shift, ΔR, against analyte concentration response curve was measured over the concentration range 1×10^{-15} M < [streptavidin] < 1×10^{-6} M and 7×10^{-10} M < [anti-biotin] < 7×10^{-6} M (Fig. 9) [20, 28]. The lines seen in Fig. 9 are not a fit to the data. Instead, the line was computed from a response model (a complete analysis of this model is described in [28]). It was found that this response could be interpreted quantitatively in terms of a model involving; (i) 1:1 binding of a ligand to a multivalent receptor with different sites but invariant affinities; and (ii) the assumption that only adsorbate-induced local refractive index changes were responsible for the operation of the LSPR nanosensor.

The binding curve provides three important characteristics regarding the system being studied. First, the mass and dimensions of the molecules affect the magnitude of the LSPR shift response. Comparison of the data with theoretical expectations yielded a saturation response, $\Delta R_{max} = 26.5$ nm for streptavidin, a 60 kDa molecule, and 38.0 nm for anti-biotin antibody, a 150 kDa molecule. Clearly, a larger mass density at the surface of the nanoparticle results in a larger LSPR response. Next, the surface-confined thermodynamic binding constant $K_{a,surf}$ can be calculated from the binding curve and is estimated to be 1×10^{11} 1/M for streptavidin and 4.5×10^7 1/M for anti-biotin antibody. These numbers are directly correlated to the third important characteristic of the system, the LOD. The LOD is less than 1 pM for streptavidin and 100 pM for anti-biotin antibody. As predicted, the LOD of the nanobiosensor studied is lower for systems with higher binding affinities such as for the well-studied biotin-streptavidin couple and higher for systems with lower binding affinities as seen in the anti-biotin antibody system. Given this information and analysis, a similar treatment can be made for virtually any ligand receptor system. It should be noted that the LOD of the system corresponds to the smallest reliable wavelength shift response induced by a given solution concentration. These 'real' LODs are often translated to the commonly reported surface coverage in terms of molecules. For the LSPR nanosensor, the surface coverage detection corresponds to ~25 streptavidin molecules per nanoparticle. In the previously described experiments, $\sim 3 \times 10^8$ nanoparticles were probed (nanoparticle density $\sim 1 \times 10^{10}$ nanoparticles per square centimetre with a spot size with a 1 mm radius), and this corresponds to the detection of a 75×10^8 streptavidin molecules. A clear method to decrease the number of molecules detected would be to decrease the number of nanoparticles probed.

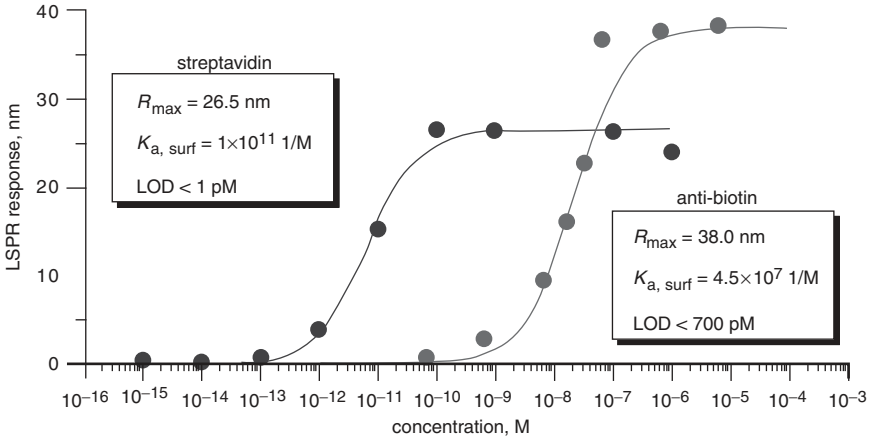

Fig. 9 *The specific binding of streptavidin (left) and anti-biotin (right) to a biotinylated Ag nanobiosensor is shown in the response curves. All measurements were collected in a N_2 environment. The solid line is the calculated value of the nanosensor's response. Reproduced with permission from [20]. Copyright 2002, The American Chemical Society. Reproduced with permission from [28]. Copyright 2003, The American Chemical Society*

This has been recently demonstrated as described in greater detail in a later Section.

3.12 Detection of disease markers using the LSPR sensor chip

Alzheimer's disease is the leading cause of dementia in people over age 65 and affects an estimated 4000 000 Americans [148]. Although first characterised almost 100 years ago by Alois Alzheimer, who found brain lesions now called plaques and tangles in the brain of a middle-aged woman who died with dementia in her early fifties [149], the molecular cause of the disease is not understood; and an accurate diagnostic test has yet to be developed. However, two inter-related theories for Alzheimer's disease have emerged that focus on the putative involvement of neurotoxic assemblies of a small 42-amino acid peptide known as amyloid beta (Aβ) [150, 151]. The widely investigated 'amyloid cascade' hypothesis suggests that the amyloid plaques cause neuronal degeneration and, consequently, memory loss and further progressive dementia. In this theory, the Aβ protein monomers, present in all normal individuals, do not exhibit toxicity until they assemble into amyloid fibrils [152]. The other toxins are known as Aβ-derived diffusible ligands ('ADDLs'). ADDLs are small, globular, and readily soluble, 3-24mers of the Aβ monomer [153] and are potent and selective central nervous system neurotoxins which possibly inhibit mechanisms of synaptic information storage with great rapidity [153]. ADDLs now have been confirmed to be greatly elevated in autopsied brains of Alzheimer's disease subjects [154]. An ultra-sensitive method for ADDLs/anti-ADDLs antibody detection potentially could emerge from LSPR nanosensor technology, providing an opportunity to develop the first clinical lab diagnostic for Alzheimer's disease. Preliminary results indicate that the LSPR nanosensor can be used to aid in the diagnosis of Alzheimer's disease [155, 156].

3.13 Sensing with single nanoparticles

The extension of the LSPR sensing technique to the single nanoparticle limit provides several improvements over existing array- or cluster-based techniques [157, 158]. First, absolute detection limits are dramatically reduced. The surface area of chemically prepared Ag nanoparticles is typically less than 20 000 nm^2, which requires that a complete monolayer of adsorbate must constitute fewer than approximately 100 zeptomol. The formation of alkanethiol monolayers on Ag nanoparticles can result in a LSPR λ_{max} shift of greater than 40 nm, a change that is over 100 times larger than the resolution of convention UV-visible spectrometers [159]. This suggests that the limit of detection for single nanoparticle-based LSPR sensing will be well below 1000 molecules for small molecule adsorbates. For larger molecules such as antibodies and proteins that result a greater change in the local dielectric environment upon surface adsorption, the single molecule detection limit may be achievable [28]. Second, the extreme sensitivity of single nanoparticle sensors dictates that only very small sample volumes (i.e. attolitres) are necessary to induce a measurable response. This characteristic could eliminate the need for analyte amplification techniques (e.g., the polymerase chain reaction) required by other analytical methods. Third, single nanoparticle sensing platforms are readily applicable to multiplexed detection schemes. By controlling the size, shape, and chemical modification of individual nanoparticles, multiple sensing platforms can be generated in which each unique nanoparticle can be distinguished from the others based on the spectral location of its LSPR [81, 157, 158]. Several of these unique nanoparticles may then be incorporated into a one device, allowing for the rapid, simultaneous detection of thousands of different chemical or biological species.

The key to exploiting single nanoparticles as sensing platforms is developing a technique to monitor the LSPR of individual nanoparticles with a reasonable signal-to-noise ratio [81]. UV-visible absorption spectroscopy does not provide a practical means of accomplishing this task. Even under the most favourable experimental conditions, the absorbance of a single nanoparticle is very close to the shot noise-governed limit of detection. Instead, resonant Rayleigh scattering spectroscopy is the most straightforward means of characterising the optical properties of individual metallic nanoparticles.

3.14 Experimental procedure for single nanoparticles

Colloidal Ag nanoparticles were prepared by reducing silver nitrate with sodium citrate in aqueous solution according to the procedure referenced above [40]. Immobilised particles on cover slips were inserted into a flow cell and were exposed to various dielectric environments or molecular adsorbates [81]. Prior to all experiments, the nanoparticles in the flow cell were repeatedly rinsed with methanol and dried under nitrogen. All optical measurements were performed using an inverted dark-field microscope equipped with an imaging spectrograph [81, 82]. The apparatus used in these experiments is shown in Fig. 10.

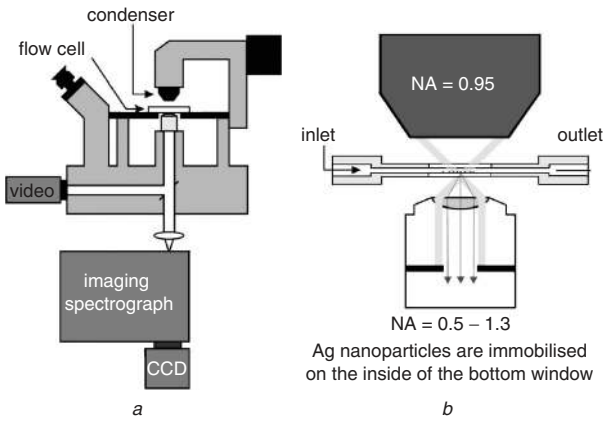

Fig. 10
a Diagram of the instrumentation used for single nanoparticle spectroscopy
b Close-up of the flow cell to show illumination and collection geometry

3.15 Single nanoparticle refractive index sensitivity

The local refractive index sensitivity of the LSPR of a single Ag nanoparticle was measured by recording the resonant Rayleigh scattering spectrum of the nanoparticle as it was exposed to various solvent environments inside the flow cell. As illustrated in Fig. 11, the LSPR λ_{max} systematically shifts to longer wavelength as the solvent RIU is increased. Linear regression analysis for this nanoparticle yielded a refractive index sensitivity of 203.1 nm RIU^{-1}. The refractive index sensitivity of several individual Ag nanoparticles was measured and typical values were determined to be 170–235 nm RIU^{-1} [81]. These are similar to the values obtained from experiments utilising arrays of NSL fabricated triangular nanoparticles [26, 84].

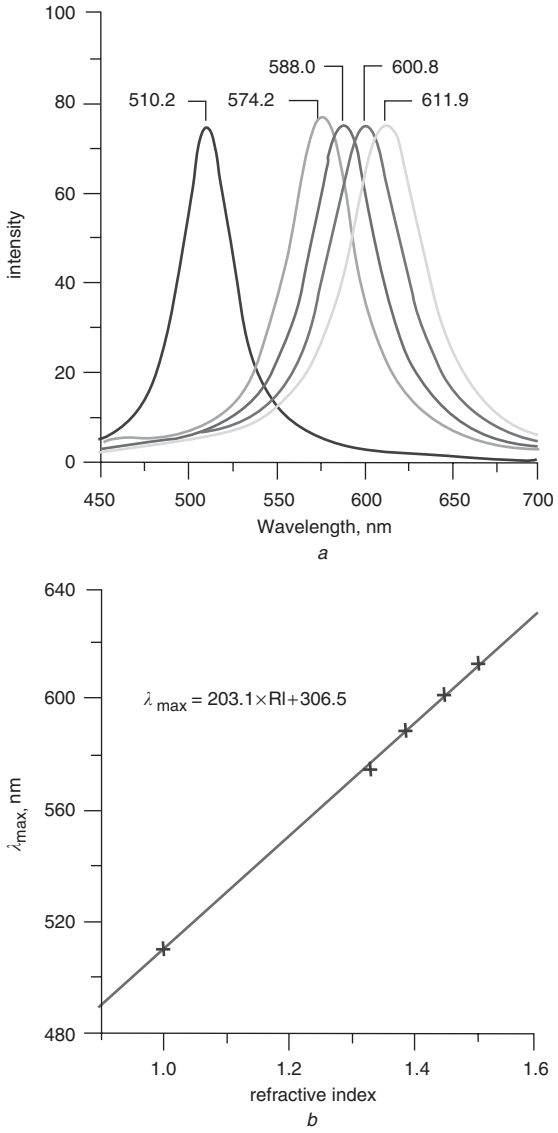

Fig. 11
a Resonant Rayleigh scattering spectra of an individual silver nanoparticle in various dielectric environments (N_2, methanol, 1-propanol, chloroform, and benzene)
b A plot depicting the linear relationship between the solvent refractive index and the nanoparticle's λ_{max}. Reproduced with permission from [81]. Copyright 2003, The American Chemical Society

3.16 Streptavidin sensing with single nanoparticles

In nanoparticle array sensing, it has been demonstrated that it is possible to detect < 100 streptavidin molecules per nanoparticle (in a solution concentration of 1 pM). The biology community would like to reduce the amount of biological sample needed for an assay without amplification. For this reason, experiments have been conducted to detect streptavidin on single Ag nanoparticles [82]. After functionalisation with a capture biomolecule, the LSPR of an individual nanoparticle was measured to be 508.0 nm (curve (i) in Fig. 12). Next, 10 nM streptavidin was injected into the flow cell, and the λ_{max} of the nanoparticle was measured at 520.7 nm, curve (ii) in Fig. 12. This + 12.7 nm shift is estimated to arise from the detection of less than 700 streptavidin molecules. It is hypothesised that just as in the array format, as the streptavidin concentration decreases, a fewer number of streptavidin molecules will bind to the surface thereby causing smaller wavelength shifts.

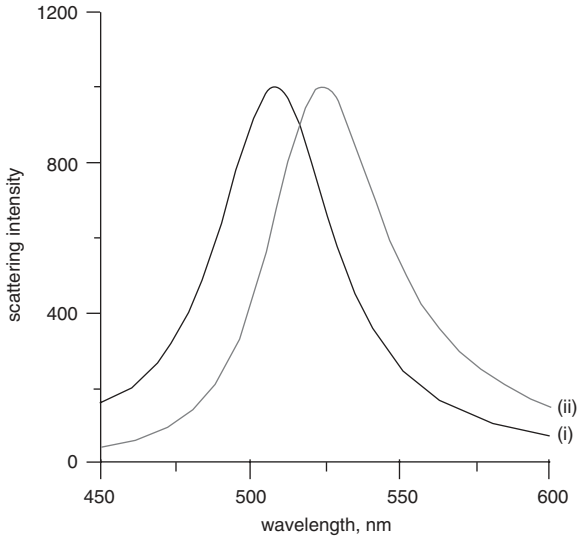

Fig. 12 *Individual Ag nanoparticle sensor before and after exposure to 10 nM streptavidin. All measurements were collected in a nitrogen environment*
(i) Biotinylated Ag nanoparticle, $\lambda_{max} = 508.0$ nm.
(ii) After streptavidin incubation, $\lambda_{max} = 520.7$ nm.

3.17 Theoretical explanation of LSPR sensing

To model the experiment results presented above, the discrete dipole approximation (DDA) method [160, 161] a finite element-based approach to solving Maxwell's equations for light interacting with an arbitrary shape/composition nanoparticle was used to calculate the plasmon wavelength in the presence or absence of an adsorbate with a wavelength-dependent refractive index layer thickness. Bare silver nanoparticles with a truncated tetrahedral shape were first constructed from cubic elements and one to two layers of the adsorbate were added to the exposed surfaces of the nanoparticle to define the presence of the adsorbate. All calculations refer to silver nanoparticles with a dielectric constant taken from Lynch and Hunter [162].

In this treatment the dielectric constant is taken to be a local function, as there is no capability for a non-local description within the DDA approach. There have been several earlier studies in which the DDA method has been calibrated by comparison with experiment for truncated tetrahedral particles, including studies of external dielectric effects and substrate effects [11, 71, 163] and based on this it is expected that DDA analysis will provide a useful qualitative description of the results. In particular, it has been demonstrated that the plasmon resonance shift close to the nanoparticle surface is dominated by hot spots while that farther away arises from colder regions around the nanoparticle surface. By comparing the overall maximum LSPR shifts of the nanoparticles, it was shown that increasing the aspect ratio of Ag nanotriangles produces larger plasmon resonances shifts and shorter-ranged interactions.

This behaviour can be easily compared to lightning rods (invented by Ben Franklin) which are placed at the top of a building, and are designed to provide a location where lightning will strike and from which the energy is carried harmlessly to the ground. A needle-like metal tip is used in a lightning rod, since this leads to high electric fields just above the tip when the building is charged relative to the atmosphere above it, providing a more likely location for lightning to strike. A similar description can be used to describe light's interaction with tips of nanoscale silver and gold nanotriangles [26, 27]. This property is best displayed

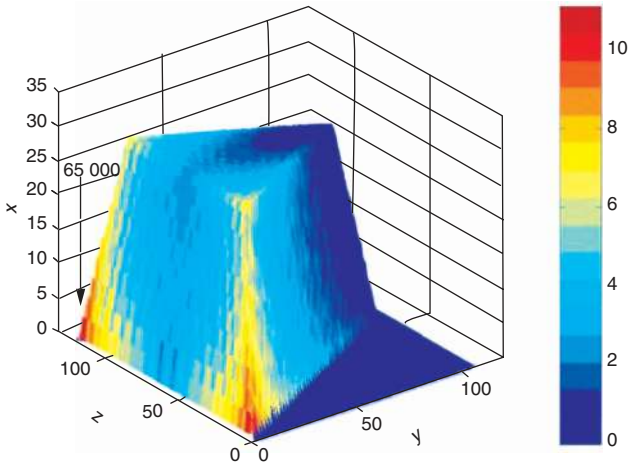

Fig. 13 *Local E-field (plotted as contours of log $|E|^2$) for a Ag nanoparticle (in-plane width = 100 nm, out-of-plane height = 30 nm). Reproduced with permission from [26]. Copyright 2004, The American Chemical Society*

in Fig. 13. This Figure was generated using the DDA method. This leads to fields around the nanoparticles whose magnitudes relative to the incident light are plotted in the Figure. The results show that the electromagnetic fields are greatly amplified (up to 65 000 times) in the region near the nanoparticle tips, leading to enhanced sensitivity to molecules that might be located there. This information can be used as a basis for constructing nanoparticle structures and understanding the sensing mechanism for surface-enhanced spectroscopies.

4 Biological applications of surface-enhanced Raman scattering

Inelastic photon scattering was first witnessed by Raman and Krishnan in 1928 [164] a process later to bear the name Raman scattering and to garner the authors a Nobel Prize in 1930. In the original Nature paper [164] the inelastic scattering effect was recognised by 'its feebleness in comparison with ordinary (Rayleigh) scattering, and by its polarisation.' Raman was able to observe this phenomenon by focusing a beam of sunlight through a telescope and a green filter, and observing the wavelength-shifted yellow light scattered from chloroform. The development of the laser, as a source of high intensity and nearly monochromatic light, enabled the more practical detection of the one inelastically scattered photon from the 10^8 elastically scattered photons [165]. Further developments in the field of photonics, such as high quality interference and notch filters, and ultra-sensitive photodetectors and CCD cameras, have enabled the routine use of Raman spectroscopy as a complement to conventional vibrational techniques such as near-infrared absorbance spectroscopy. As a vibrational spectroscopy, Raman scattering generates information rich spectra unique to a given molecule [165]. The potential to use the unique molecular information to perform optical 'fingerprinting' capable of distinguishing almost any analyte by its spectroscopic signature alone has interested analytical chemists and biologists for years. Researchers have striven to overcome the low scattering cross-sections inherent in normal Raman spectroscopy (NRS) which is a process approximately a million-fold less efficient than fluorescence, and have developed a number of impressive biological applications. For example, NRS has been used in the detection of glucose, in proteomics, the diagnosis of cancer and cardiovascular health, the identification of small molecule drugs, and so forth. Reviews of these applications have recently been written by Cotton *et al.* [166], Nabiev *et al.* [167], and Petry *et al.* [168]. However, the low signal intensities and complications with spectral identification caused by the generation of a spectral response all species in a complex mixture and the concomitant confusion generated by closely spaced or overlapping Raman bands unfortunately hinder application of NRS. SERS can increase the scattering cross-section of a molecule in proximity to a nanoscale roughened surface by 10^6 to 10^{14} times, potentially mitigating the two aforementioned disadvantages of NRS [169, 170].

SERS is a plasmonic phenomenon whereby specific molecules at or near a nanoscale roughed metal surface undergo a dramatic increase in the intensity of the observed inelastically scattered light. Since the discovery of SERS by Jeanmaire and Van Duyne [171] the exact mechanism of enhancement has remained controversial [172, 173]. However, it is generally agreed that two mechanisms contribute to the overall enhancement, a chemical effect (CHEM, α) and an electromagnetic (EM, E) enhancement. The intensity of Raman scattering is proportional to the square of P, the electric field-induced dipole moment. The P term is related to the molecular polarisablity (α) and the electric field (E) experienced by the molecule. These relationships are mathematically expressed thus:

$$G \propto P^2 \tag{4}$$

and

$$P = \alpha E \tag{5}$$

The electromagnetic effect gives rise to an enhanced Raman yield for a given molecular polarisability, whereas the chemical effect refers to a change in the polarisability itself. The theory of chemical enhancement (α) was invoked to account for a discrepancy between the enhancement predicted the electrical model (E) ($\sim 10^4$) and the empirically determined enhancement ($\sim 10^6$). It is thought that 'active sites', either crystal defects or adatoms on the surface of the metal surface undergo a charge-transfer process enabling the CHEM (α) enhancement [170]. The dependence of optimal SERS excitation frequency on the electrode potential suggests that new electronic states may arise upon adsorption of the analyte, which leads to resonant intermediate states for Raman scattering. The CHEM enhancement has been investigated, particularly the effect of halide ions on increasing SERS [173–176]. The recent discovery of single molecule SERS (SMSERS) by Nie and Emory [177] and Kneipp *et al.* [178] in 1997, has necessitated further refinements to the EM mechanism.

It is well established that the EM mechanism arises from optical excitation of surface plasmon resonances in small metal particles, which leads to a significant increase in the electromagnetic field strength at the particle surface. Initially, Moskovits [179] developed a resonant fractal theory to explain surface Raman enhancement in extensively aggregated colloids. For single particles and small aggregates, however, the case can be dramatically different than for an ensemble average of particles. Electromagnetic enhancement is attributable to the formation a LSPR, as described above. This polarises the particle with an electromagnetic field significantly higher than the applied field. Recent theoretical modelling, has greatly extended the nature of the plasmonic material (e.g. particle morphology, spacing, and coupling) beyond the simple spherical model developed by Mie, and is more useful in describing actual experimental conditions. The intensified field at rough or highly-curved surfaces enhances both the incident laser light

and the scattered Raman light. Due to the dependence of the SERS signal intensity on the fourth-power of the EM field, the signal drops by a factor of ten for each nanometre separation between the molecule and the surface [180–182]. This electromagnetic enhancement can be qualitatively conceptualised as an 'antenna' effect, gathering and strengthening local electric fields.

4.1 Intrinsic SERS of target molecules

SERS provides not only enhanced signal intensities but also species specific spectra, so it is therefore unsurprising that many SERS experiments have been conducted that attempt to directly address molecules of biological interest and their chemical interactions. The first such experiment was conducted in 1980 by Cotton *et al.* on cytochrome *c* and hemoglobin, molecules with strong electronic absorbances in the visible. These intense absorbances were matched with the laser excitation wavelength, λ_{ex}, to eke out a few orders of magnitude extra enhancement by exploiting surface-enhanced resonance Raman spectroscopy (SERRS). The resonance effect has continued to make hemoglobin and cytochrome *c* popular proteins for study, particularly since the advent of SMSERS [183, 184]. In the same year as Cotton's pioneering experiments, Billman and Otto [185] also demonstrated the successful detection of cyanide on roughened silver electrodes [188]. Cyanide, while not a biomolecule as such, is nonetheless of great interest in both biological, environmental, and defence circles in the detection of cyanides and similar molecules which have a direct impact on biological systems. As another example, SERS has been used on the bio-terror front for the detection of anthrax [186]. SERS has been demonstrated to successfully detect dipicolinic acid, the principle chemical component of *bacillus anthracis* spores (15% wt) [187]. Since the 1980s, the number of biological applications of SERS (and NRS) has skyrocketed [166–168, 188–194]. Indeed significant strides have been made in the Raman spectroscopy of proteins and peptides using NRS, and progress continues as the use of SERS expands. SERS techniques have been applied to an impressive variety of systems [193, 195–207]. Initially, most SERS experiments were conducted on electrochemically roughened surfaces. However, since the discovery of SMSERS, researchers have increasingly tended to use colloidal systems as they are easy to prepare chemically and to model theoretically. Exceptions are common, however, Maxwell *et al.* [208] employed size-selected nanoparticle films to study amoxicillin and adenine, and the metal film-over-nanosphere (MFON) surfaces remain popular for their mechanical stability [209]. Remarkably, Kneipp *et al.* [210] have been able to obtain SERS spectra from gold nanoparticles sited within single living cells. Recently, Jarvis and Goodacre [211] have used SERS on aggregated silver colloids in combination with chemometric techniques to classify a collection of clinical bacterial isolates. SERS can also be used to study molecular interactions and dynamics, such a protein interactions [212–214] and pharmacokinetics [162, 215, 216]. Naturally, both SERS and NRS lend themselves to sensitive detection modalities for separation science [216–219].

4.2 SMSERS

Despite its tremendous power and potential the capricious nature of SMSERS has resulted in only a few publications on its biological application. In 1998, Kneipp et al. [220] were the first to successfully obtain SERS spectra from single nucleoside bases building on their experience with not only SMSRS [178] but also SERS detection of DNA [221, 222]. Shortley afterwards, Keller *et al.* [223] and Emory and Keller [224] brought SMSERS to bear on nucleosides. Recently, Xu et al. [225] have returned to the use of hemoglobin as the SERS analyte, but at the single molecule level. This 1999 study was augmented a year later by an excellent manuscript covering the contribution of the EM mechanism of SMSERS [226]. Since then, these researchers have combined SMSERS with fluorescence correlation spectroscopy to study HRP: a highly useful component in the bioanalytical toolkit [227]. SMSERS on myoglobin has reported by Bizzarri and Cannistraro [228] while Habuchi *et al.* [229] obtained SERRS spectra from the green fluorescent protein.

4.3 Limitations to intrinsic SERS

There are two considerable difficulties in applying SERS directly to biological problems. First, without resonance enhancement (as in the case of cytochrome *c*) it is still often difficult to obtain quality Raman spectra of biologically interesting molecules (e.g. drugs, protein, nucleic acids, etc.), particularly at the relatively low concentrations often necessitated by the expense or insolubility of the analyte. Even although SERS is potentially sensitive for single molecule spectroscopy, not all molecules, such as water, are efficient SERS scatterers. Also many molecules neither adsorb nor bind to the SERS active surface, making them difficult to detect, given the consequent lack of chemical (CHEM) enhancement and greatly diminished electromagnetic enhancement (EM). Approximately one-order of magnitude in SERS intensity is lost per nanometre distance the target molecule is from the enhancing substrate, making the detection of certain molecules, such as some ionic species, carbohydrates, etc., particularly problematic. Second, large biomacromolecules and numerous small molecules of biological importance have complex Raman spectra, and often have a number of overlapping peaks due to structural similarities in the molecule. For example all biomacromolecules are built from a limited set of building blocks; the approximately 20 amino acids for proteins, and eight nucleic acids for DNA and RNA. Teasing out specific information about a given biomacromolecule and its composition, conformation, or interactions is a particularly daunting, but not impossible task. The problem becomes particularly difficult in complex mixtures, which are the norm for biologically interesting systems such as environmental samples from contaminated waste sites, and the protein jungle of the cytosol.

4.4 Extrinsic SERS labelling

Several approaches have been reported to address the difficulties with direct SERS-based detection of biologically relevant targets. An attractive option is to indirectly detect the presence of interaction of a complex and/or weakly scattering molecule by labelling it with a small molecule with high intensity, well defined, and characteristic spectral features [230, 231]. The extrinsic labelling schemes described below are all variations on the ELISA (enzyme-linked immunosorbent assay). A graphical summary of the various extrinsic SERS methods is shown in Fig. 14. In a standard ELISA, molecular binding events are detected using antibodies (Abs) possessing a high affinity for the molecule of interest, and which are covalently bound to an enzyme (e.g. HRP). Once the target molecule is immobilised on a surface, the target is exposed to the detection AB/enzyme complex. The substrate for the enzyme is then introduced, and the enzymatic reaction allowed to occur. Typically the product of the enzymatic reaction is then detected by a change in a physical property, such a colour for HRP/OPD (ortho-phenylenediamine). The amount of target is

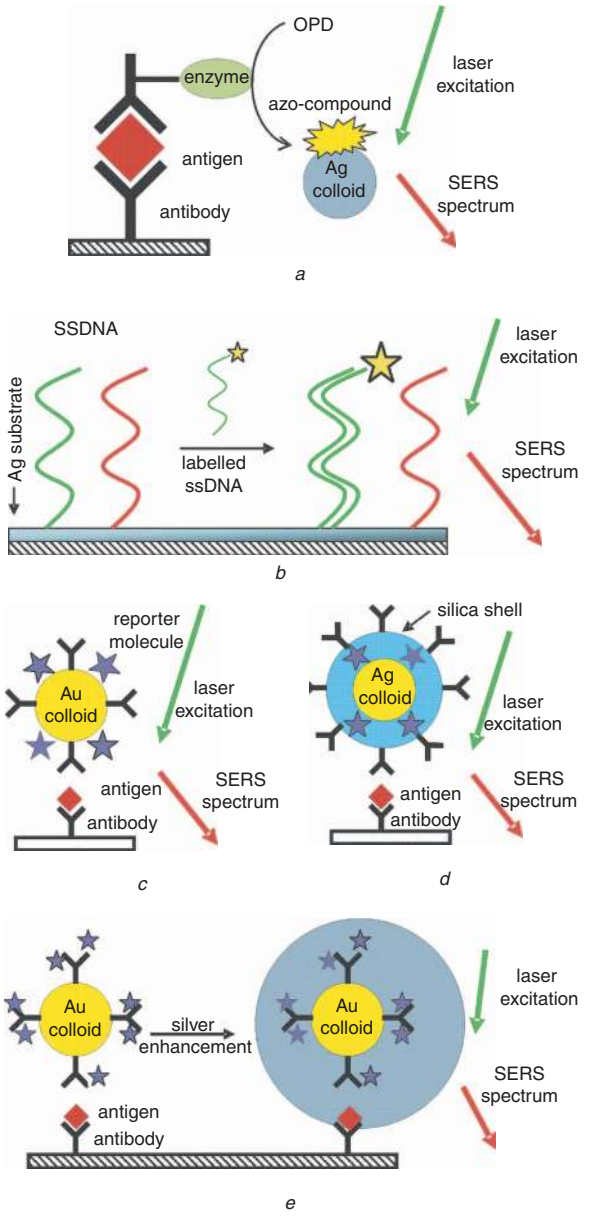

Fig. 14 *Schematic of extrinsic SERS labeling methods*
a SERS used to detect enzyme reaction product.
b Detection of a labelled DNA after hybridisation to capture ssDNA bound to a silver substrate
c Extrinsic Raman Labels (ERLs) formed by the co-addition of a Raman reporter and protein to gold colloid
d Composite nanospheres with encapsulated Raman labels and protective silica shell
e Silver-enhanced SERS detection with protein-modified gold probes acting as nucleation sites for electroless silver deposition

therefore proportional to the intensity of the colour produced after a set period of time. Dou et al. [232] were the first to adapt an ELISA-type assay by replacing chromogenic read out with SERS detection. Vo-Dinh and co-workers deposited silver metal on the surface of DNA chips and demonstrated that SERS spectra could be obtained from dye-labelled gene probes [233–235]. Using colloidal nanoparticles, Graham *et al.* [236, 237] reported multiplexed SERS detection of labelled polymerase chain reaction products, and Ni *et al.* [238] and Pham *et al.* [239] showed that colloidal gold with co-adsorbed organic molecules and Ab could be used for immunoassay readout. Improvements were realised for this method by using larger, but more optimally enhancing 63 nm gold nanoparticles, which had stronger spectral intensities and were intense enough to permit single particle imaging [240]. Innovative results have also been reported by Mulvaney *et al.* [241] and Doering and Nie [175] who prepared silica encapsulated nanoparticles for use in multiplexed bioassays. These encapsulated particles are stable in the presence of high salt (common in most biological buffers), and the silica shell protects not only the particle from the environment, but also the environment from the potentially toxic Raman reporter. In a significant departure from traditional SERS substrates, Cao *et al.* [242] prepared SERS-active nanostructures by seeded growth of silver on gold and demonstrated that these structures are useful for multiplexed nucleic acid detection. The seeded growth method was extended to protein detection and labelling in [243] and cell and tissue labelling in lab [99]. Both methods use small gold nanoparticles associated with both a reporter molecule for signal specificity and protein to confer biological activity [244]. After binding of the bioconjugates to the target, electroless deposition is employed to develop a shell of silver metal around the nanoparticle seed, in a process confusingly referred to as 'silver enhancement'. The silver layer forms a complex fractal surface, providing the nanoscale roughness necessary for efficient SERS. Whereas Cao *et al.* [242] synthesised reporter-labelled DNA/protein conjugates, the method developed by Stuart et al. [99] functionalises amine reactive dye molecules directly onto existing protein gold bioconjugates. This later method not only is simpler and substantially less expensive, but also leads to higher reporter and protein levels which increases both the conjugate's binding capacity and observed signal intensity.

4.5 Spectroscopic labelling of biological samples with enhanced probes

Since Raman scattering can be semi-quantitative, and does not photobleach, this method may prove useful to many biomedical researchers, for example, to those studying cancer. As a test bed, the technology was applied to tissue sections in a microarray format. Colon cancer/normal tissue microarrays were purchased from Zymed Laboratories Inc., and subsequently deparaffinised and re-hydrated according to the manufacturer's protocol. Primary antibody (mouse anti-carcinoembryonic antigen, CEA) conjugation was achieved by following the manufacturer's protocol, which could readily be automated. Secondary labelling with malachite green/anti-mouse gold particles and subsequent silver enhancement was performed as per standard immunogold and silver staining practice [245]. The limiting factor is not the spectroscopy, which is capable of single molecule sensitivity and large number of strongly SERS-active reporters for multiplexing, but the availability of suitably specific biomolecules. Fortunately, the CEA antibody binds to a wide range of colon cancer types, but has minimal interaction with normal tissue. Figure 15 shows the ability of the technology to discriminate between the cancerous tissues (red line) and tissues taken near (adjacent mucosa, blue line) and far from the tumor site (remote mucosa, black line). By recording the spectrum of the marking tissue, the 'hump' was eliminated by background subtraction. Also, the silver staining itself provides a rapid method of determining if particles were successfully bound, and serves as a secondary method of staining tissues [246]. Figure 15 shows, however, that the level of staining required to generate a SERS signal is quite low. To the unaided eye, there is no difference between the normal (Fig. 15*b*) and the cancer tissue sections (Fig. 15*c*). Even under microscopic examination, correctly identifying the silver-enhanced sections of the tissue can require skill and training. Spectroscopic labelling provides a rapid and unambiguous

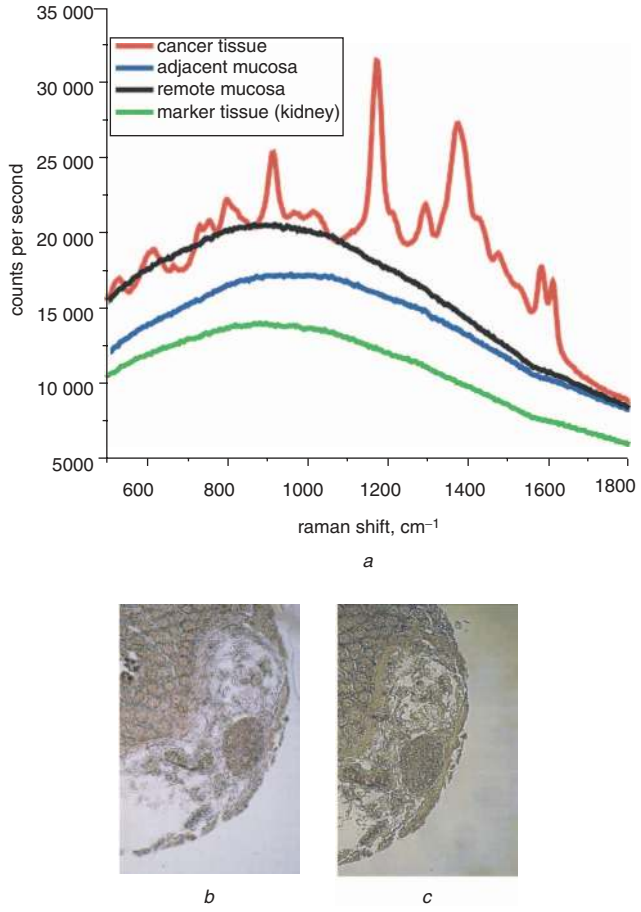

Fig. 15
a Spectroscopic identification of cancer tissue. Spectra from cancerous tissue (red), adjacent mucosa (blue), remote mucosa (>6 cm distant) (black), after secondary labelling with nanoparticle/dye conjugates and subsequent silver enhancement. The cancerous tissue display clear and distinct peaks indicating positive labelling with the nanoparticle probes, whereas the control tissues show broad, featureless spectra
b Photomicrograph of cancer tissue before the silver enhancement process
c Photomicrograph of normal tissue after the silver enhancement process

differentiation, and the operator familiarisation time for the instrument would be minimal.

4.6 SERS using functionalised substrates

A secondary method of overcoming the difficulty in the direct SERS detection of problematic analytes is to employ a functionalised SERS surface. By coating the SERS active substrate with a SAM [247], hydro-gel [248] or polymer [249] substantial gains in signal can be realised from analytes whose SERS spectra are otherwise difficult or impossible to obtain. Whereas the specifics of the interactions between the functionalised surface and the complex mixture are inherently unique to each particular combination of analyte and surface, two general mechanisms operate simultaneously to provide the improved signal.

First, the material coating the SERS substrate can act as a barrier to undesired analytes. In this sense, the coating layer acts as a chemical and physical filter. For example, large species may be effectively excluded by controlling the pore size on a polymer substrate coating, or cations may be repelled by using a charged SAM bound to a SERS active surface. Stokes *et al.* [249] recognised the potential of combining polymers with SERS. The technique of SAM functionalisation has been largely pioneered by [203, 218, 250–252] who have used the selectivity of the SAM in the analysis of bilirubins and salicalate from whole blood, and drug compounds amongst other targets. From a biomedical and device perspective, perhaps the most interesting application of this selective SAM approach has been the detection glucose by the collaborative efforts at Northwestern University [253, 254].

4.7 SERS detection of glucose

The NIH estimates on the number of diabetics in the US is staggering. An estimated 17 000 000 people, or about 7% of the US population suffer from diabetes. Current treatment of diabetes consists of self-regulation of blood glucose levels through frequent 'finger-stick' monitoring. A faster, easier, automated, and less painful method for frequently measuring glucose levels would be of great individual, clinical, and societal benefit.

AgFONs with a monolayer of EG3 (Fig. 16*a*) were incubated for 1 h in glucose solutions (0–25 mM) of clinically relevant concentrations. SERS spectra were then measured from each sample. The chemometric method of partial least squares (PLS) is used when the spectrum of an analyte of interest is embedded within a complex background spectrum [255]. The result of PLS analysis is a plot

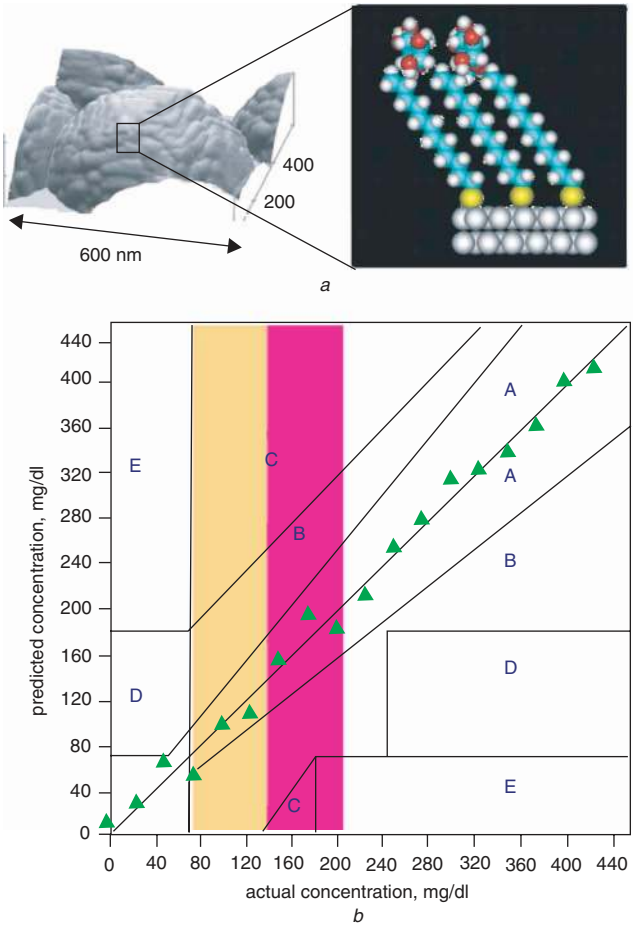

Fig. 16
a Schematic showing hypothetical glucose concentration gradient created by a partition layer.
b Plot of PLS predicted physiologically relevant glucose concentrations vs against actual glucose concentrations using leave-one-out cross-validation projected on a Clark Error grid. AgFON samples were made (sphere diameter = 390 nm, metal thickness = 200 nm), incubated for 19 hs in 1 mM EG3, and dosed in glucose solution (range: 0–25 mM) for 10 min. Each SERS measurement was made while samples were in an environmental control cell filled with glucose solution, using $\lambda_{ex} = 632.8$ nm (3.25 mW, 30 s). Dashed line is not a fit, but rather represents a perfect prediction

of predicted analyte concentration against actual analyte concentration. As shown in Fig. 16*b*, the SERS transduction mechanism successfully predicts glucose concentration quantitatively, with the vast majority of the data points falling within the A or B areas of the Clark-error grid [256].

5 Conclusions

We have highlighted representative research accomplishments in the area of the tunable LSPR of silver and gold nanoparticles in solution and on surfaces and the application of two unique plasmonic phenomenonae (i.e. the LSPR and SERS) to biological applications and systems. We have provided the reader with a sufficiently deep, yet accessible, coverage of the underlying principles and theory behind surface plasmonics and its application to nanobioanalysis. We have highlighted work in the field that is not only relevant and innovative, but also shows immediate promise for near-term implementation in real-world applications such as point-of-care diagnostics, environmental monitoring, proteomics, drug discovery, and fundamental biological research. Future commercialisation of nanoparticle devices relies on a better understanding of the interaction between nanoparticles and their immediate environment, as well as the development of techniques that will preserve nanoparticle optical activity under challenging biological conditions.

6 Acknowledgments

We gratefully acknowledge financial support from the Nanoscale Science and Engineering Initiative of the National Science Foundation under NSF award EEC-0118025. Any opinions, findings, and conclusion or recommendations expressed in this material are those of the authors and do not necessarily reflect those of the National Science Foundation. A. Haes acknowledges the ACS division of Analytical Chemistry sponsored by DuPont for fellowship support. This project was also supported by the Institute for Bioengineering and Nanoscience in Advanced Medicine at Northwestern University, and the National Institutes of Health (EY13002 and EY13015). The authors wish to thank the following individuals for their experimental assistance, materials, or expertise: L. Chang, W. E. Doering, M. Glucksberg, N. Halas, W. P. Hall, C. L. Haynes, E. Jeoung, M. Käll, W. L. Klein, O. Lyandres, M. Mrksich, C. Murphy, A. D. McFarland, S. Nie, J. C. Riboh, G. C. Schatz, K. Shafer-Peltier, J. Walsh, Y. Xia, and S. Zou.

7 References

1 Haynes, C.L., and Van Duyne, R.P.: 'Nanosphere Lithography: A Versatile Nanofabrication Tool for Studies of Size-Dependent Nanoparticle Optics', *J. Phys. Chem. B*, 2001, **105**, pp. 5599–5611
2 Mulvaney, P.: 'Not all that's gold does glitter', *MRS Bull.*, 2001, **26**, pp. 1009–1014
3 El-Sayed, M.A.: 'Some Interesting Properties of Metals Confined in Time and Nanometer Space of Different Shapes', *Accounts Chem. Res.*, 2001, **34**, pp. 257–264
4 Link, S., and El-Sayed, M.A.: 'Spectral Properties and Relaxation Dynamics of Surface Plasmon Electronic Oscillations in Gold and Silver Nano-dots and Nano-rods', *J. Phys. Chem. B*, 1999, **103**, pp. 8410–8426
5 Kreibig, U., Gartz, M., Hilger, A., and Hovel, H.: 'Optical investigations of surfaces and interfaces of metal clusters', *in* Duncan, M.A. (ed.): 'Advances in Metal and Semiconductor Clusters' (JAI Press Inc., Stamford, , 1998), Vol. 4, pp. 345–393
6 Mulvaney, P.: 'Surface Plasmon Spectroscopy of Nanosized Metal Particles', *Langmuir*, 1996, **12**, pp. 788–800
7 Kreibig, U.: 'Optics of nanosized metals', *in* Hummel, R. E. and Wissmann, P. (Eds.) 'Handbook of Optical Properties' (CRC Press, Boca Raton FL, 1997), Vol. II, pp. 145–190
8 Hulteen, J.C., Treichel, D.A., Smith, M.T., Duval, M.L., Jensen, T.R., and Van Duyne, R.P.: 'Nanosphere Lithography: Size-Tunable Silver Nanoparticle and Surface Cluster Arrays', *J. Phys. Chem. B*, 1999, **103**, pp. 3854–3863
9 Freeman, R.G., Grabar, K.C., Allison, K.J., Bright, R.M., Davis, J.A., Guthrie, A.P., Hommer, M.B., Jackson, M.A., Smith, P.C., Walter, D.G., and Natan, M.J.: 'Self-Assembled Metal Colloid Monolayers: An Approach to SERS Substrates', *Science*, 1995, **267**, pp. 1629–1632
10 Kahl, M., Voges, E., Kostrewa, S., Viets, C., and Hill, W.: 'Periodically structured metallic substrates for SERS', *Sens. Actuators B, Chem.*, 1998, **51**, pp. 285–291
11 Schatz, G.C., and Van Duyne, R.P.: 'Electromagnetic Mechanism of Surface-Enhanced Spectroscopy', (Wiley, New York, , 2002), Vol. 1
12 Haynes, C.L., and Van Duyne, R.P.: 'Plasmon-Sampled Surface-Enhanced Raman Excitation Spectroscopy', *J. Phys. Chem. B*, 2003, **107**, pp. 7426–7433
13 Haynes, C.L., McFarland, A.D., Zhao, L., Van Duyne, R.P., Schatz, G.C., Gunnarsson, L., Prikulis, J., Kasemo, B., and Käll, M.: 'Nanoparticle Optics: The Importance of Radiative Dipole Coupling in Two-Dimensional Nanoparticle Arrays', *J. Phys. Chem. B*, 2003, **107**, pp. 7337–7342
14 Dirix, Y., Bastiaansen, C., Caseri, W., and Smith, P.: 'Oriented Pearl-Necklace Arrays of Metallic Nanoparticles in Polymers: A New Route Toward Polarization-Dependent Color Filters', *Adv. Mater.*, 1999, **11**, pp. 223–227
15 Haynes, C.L., and Van Duyne, R.P.: 'Dichroic Optical Properties of Extended Nanostructures Fabricated Using Angle-Resolved Nanosphere Lithography', *Nano Lett.*, 2003, **3**, pp. 939–943
16 Maier, S.A., Brongersma, M.L., Kik, P.G., Meltzer, S., Requicha, A.A.G., and Atwater, H.A.: 'Plasmonics-A Route to Nanoscale Optical Devices', *Adv. Mater.*, 2001, **13**, pp. 1501–1505
17 Maier, S.A., Kik, P.G., Atwater, H.A., Meltzer, S., Harel, E., Koel, B.E., and Requicha, A.A.G.: 'Local detection of electromagnetic energy transport below the diffraction limit in metal nanoparticle plasmon waveguides', *Nature Mater.*, 2003, **2**, pp. 229–232
18 Shelby, R.A., Smith, D.R., and Schultz, S.: 'Experimental verification of a negative index of refraction', *Science*, 2001, **292**, pp. 77–78
19 Andersen, P.C., and Rowlen, K.L.: 'Brilliant optical properties of nanometric noble metal spheres, rods, and aperture arrays', *Appl. Spectrosc.7*, 2002, **56**, pp. 124A–135A
20 Haes, A.J., and Van Duyne, R.P.: 'A Nanoscale Optical Biosensor: Sensitivity and Selectivity of an Approach Based on the Localized Surface Plasmon Resonance Spectroscopy of Triangular Silver Nanoparticles', *J. Am. Chem. Soc.*, 2002, **124**, pp. 10596–10604
21 Mucic, R.C., Storhoff, J.J., Mirkin, C.A., and Letsinger, R.L.: 'DNA-Directed Synthesis of Binary Nanoparticle Network Materials', *J. Am. Chem. Soc.*, 1998, **120**, pp. 12674–12675
22 Hirsch, L.R., Jackson, J.B., Lee, A., Halas, N.J., and West, J.L.: 'A Whole Blood Immunoassay Using Gold Nanoshells', *Anal. Chem.*, 2003, **75**, pp. 2377–2381
23 Haes, A.J., and Van Duyne, R.P.: 'A Highly Sensitive and Selective Surface-Enhanced Nanobiosensor', *Mater. Res. Soc. Symp. Proc.*, 2002, **723**, pp. O3.1.1–O3.1.6
24 Haes, A.J., and Van Duyne, R.P.: 'Nanosensors Enable Portable Detectors for Environmental and Medical Applications', *Laser Focus World*, 2003, **39**, pp. 153–156
25 Haes, A.J., and Van Duyne, R.P.: 'Nanoscale optical biosensors based on localized surface plasmon resonance spectroscopy', *Proc. SPIE-Int. Soc. Opt. Eng.*, 2003, **5221**, pp. 47–58
26 Haes, A.J., Zou, S., Schatz, G.C., and Van Duyne, R.P.: 'Nanoscale Optical Biosensor: Short Range Distance Dependence of the Localized Surface Plasmon Resonance of Noble Metal Nanoparticles', *J. Phys. Chem. B*, 2004, **108**, pp. 6961–6968
27 Haes, A.J., Zou, S., Schatz, G.C., and Van Duyne, R.P.: 'A Nanoscale Optical Biosensor: The Long Range Distance Dependence of the Localized Surface Plasmon Resonance of Noble Metal Nanoparticles', *J. Phys. Chem. B*, 2004, **108**, pp. 109–116
28 Riboh, J.C., Haes, A.J., McFarland, A.D., Yonzon, C.R., and Van Duyne, R.P.: 'A Nanoscale Optical Biosensor: Real-Time Immunoassay in Physiological Buffer Enabled by Improved Nanoparticle Adhesion', *J. Phys. Chem. B*, 2003, **107**, pp. 1772–1780
29 Fritzsche, W., and Taton, T.A.: 'Metal nanoparticles as labels for heterogeneous, chip-based DNA detection', *Nanotechnology*, 2003, **14**, pp. R63–R73
30 Aizpurua, J., Hanarp, P., Sutherland, D.S., Kall, M., Bryant, G.W., and Garcia de Abajo, F.J.: 'Optical Properties of Gold Nanorings', *Phys. Rev. Lett.*, 2003, **90**, pp. 057401/1–057401/4
31 Obare, S.O., Hollowell, R.E., and Murphy, C.J.: 'Sensing Strategy for Lithium Ion Based on Gold Nanoparticles', *Langmuir*, 2002, **18**, pp. 10407–10410
32 Nath, N., and Chilkoti, A.: 'Immobilized gold nanoparticle sensor for label-free optical detection of biomolecular interactions', *Proc. SPIE-Int. Soc. Opt. Eng.*, 2002, **4626**, pp. 441–448
33 Nam, J.-M., Thaxton, C.S., and Mirkin, C.A.: 'Nanoparticle-based bio-bar codes for the ultrasensitive detection of proteins', *Science*, 2003, **301**, pp. 1884–1886
34 Bailey, R.C., Nam, J.-M., Mirkin, C.A., and Hupp, J. T.: 'Real-time multicolor DNA detection with chemoresponsive diffraction

gratings and nanoparticle probes', *J. Am. Chem. Soc.*, 2003, **125**, pp. 13541–13547
35 Kreibig, U., and Vollmer, M.: 'Cluster Materials', (Springer-Verlag, Heidelberg, Germany, 1995), Vol. **25**
36 Jensen, T.R., Malinsky, M.D., Haynes, C.L., and Van Duyne, R.P.: 'Nanosphere Lithography: Tunable Localized Surface Plasmon Resonance Spectra of Silver Nanoparticles', *J. Phys. Chem. B*, 2000, **104**, pp. 10549–10556
37 Michaels, A.M., Nirmal, M., and Brus, L.E.: 'Surface Enhanced Raman Spectroscopy of Individual Rhodamine 6G Molecules on Large Ag Nanocrystals', *J. Am. Chem. Soc.*, 1999, **121**, pp. 9932–9939
38 Schultz, S., Smith, D.R., Mock, J.J., and Schultz, D.A.: 'Single-target molecule detection with nonbleaching multicolor optical immunolabels', *Proc. Natl. Acad. Sci., USA*, 2000, **97**, pp. 996–1001
39 Yguerabide, J., and Yguerabide, E.E.: 'Light-scattering submicroscopic particles as highly fluorescent analogs and their use as tracer labels in clinical and biological applications – II. Experimental characterization', *Anal. Biochem.*, 1998, **262**, pp. 157–176
40 Lee, P.C., and Meisel, D.: 'Adsorption and surface-enhanced Raman of dyes on silver and gold sols', *J. Phys. Chem.*, 1982, **86**, pp. 3391–3395
41 Frens, G.: *Nature (Phys. Sci.)*, 1973, **241**, pp. 20–22
42 Jana, N.R., Gearheart, L., and Murphy, C.J.: 'Wet chemical synthesis of high aspect ratio cylindrical gold nanorods', *J. Phys. Chem. B*, 2001, **105**, pp. 4065–4067
43 Murphy, C.J., and Jana, N.R.: 'Controlling the aspect ratio of inorganic nanorods and nanowires', *Adv. Mater.*, 2002, **14**, pp. 80–82
44 Kim, F., Song, J. H., and Yang, P.D.: 'Photochemical synthesis of gold nanorods', *J. Am. Chem. Soc.*, 2002, **124**, pp. 14316–14317
45 Sun, Y., Mayers, B., Herricks, T., and Xia, Y.: 'Polyol Synthesis of Uniform Silver Nanowires: A Plausible Growth Mechanism and the Supporting Evidence', *Nano Lett.*, 2003, **3**, pp. 955–960
46 Jin, R., Cao, Y.W., Mirkin, C.A., Kelly, K.L., Schatz, G.C., and Zheng, J.G.: 'Photoinduced conversion of silver nanospheres to nanoprisms', *Science*, 2001, **294**, pp. 1901–1903
47 Jin, R., Cao, Y.C., Hao, E., Metraux, G.S., Schatz, G.C., and Mirkin, C.A.: 'Controlling anisotropic nanoparticle growth through plasmon excitation', *Nature*, 2003, **425**, pp. 487–490
48 Maillard, M., Giorgio, S., and Pileni, M.P.: 'Tuning the size of silver nanodisks with similar aspect ratios: Synthesis and optical properties', *J. Phys. Chem. B*, 2003, **107**, pp. 2466–2470
49 Maillard, M., Giorgio, S., and Pileni, M.P.: 'Silver nanodisks', *Adv. Mater.*, 2002, **14**, p. 1084
50 Hao, E.C., Kelly, K.L., Hupp, J.T., and Schatz, G.C.: 'Synthesis of silver nanodisks using polystyrene mesospheres as templates', *J. Am. Chem. Soc.*, 2002, **124**, pp. 15182–15183
51 Sun, Y.G., and Xia, Y.N.: 'Shape-controlled synthesis of gold and silver nanoparticles', *Science*, 2002, **298**, pp. 2176–2179
52 Hao, E., Bailey, R.C., Schatz, G.C., Hupp, J.T., and Li, S.Y.: 'Synthesis and optical properties of "branched" gold nanocrystals', *Nano Lett.*, 2004, **4**, pp. 327–330
53 Yun, M.H., Myung, N.V., Vasquez, R.P., Lee, C.S., Menke, E., and Penner, R.M.: 'Electrochemically grown wires for individually addressable sensor arrays', *Nano Lett.*, 2004, **4**, pp. 419–422
54 Walter, E.C., Zach, M.P., Favier, F., Murray, B.J., Inazu, K., Hemminger, J.C., and Penner, R.M.: 'Metal nanowire arrays by electrodeposition', *Chemphyschem*, 2003, **4**, pp. 131–138
55 Penner, R.M.: 'Special issue - Electrochemistry of nanosized systems - Preface', *J. Electroanal. Chem.*, 2002, **522**, pp. 1–1
56 Kohli, P., Wirtz, M., and Martin, C.R.: 'Nanotube membrane based biosensors', *Electroanalysis*, 2004, **16**, pp. 9–18
57 Martin, C.R., and Mitchell, D.T.: 'Template-synthesized nanomaterials in electrochemistry', 'Electroanalytical Chemistry' (Marcel Dekker, New York, 1999), Vol. **21**, pp. 1–74
58 McFarland, A.D.: 'Using Nanoparticle Optics for Ultrasensitive Chemical Detection and Surface-Enhanced Spectroscopy', 'Chemistry' (IL Northwestern University, Evanston, 2004), p. 256
59 Cao, Y.W., Jin, R., and Mirkin, C.A.: 'DNA modified core-shell Ag/Au nanoparticles', *J. Am. Chem. Soc.*, 2001, **123**, pp. 7961–7962
60 Schierhorn, M., and Liz-Marzan, L.M.: 'Synthesis of bimetallic colloids with tailored intermetallic separation', *Nano Lett.*, 2002, **2**, pp. 13–16
61 Ung, T., Liz-Marzan, L.M., and Mulvaney, P.: 'Controlled method for silica coating of silver colloids. Influence of coating on the rate of chemical reactions', *Langmuir*, 1998, **14**, pp. 3740–3748
62 Alejandro-Arellano, M., Ung, T., Blanco, A., Mulvaney, P., and Liz-Marzan, L.M.: 'Silica-coated metals and semiconductors. Stabilization and nanostructuring', *Pure Appl. Chem.*, 2000, **72**, pp. 257–267
63 Ung, T., Liz-Marzan, L.M., and Mulvaney, P.: 'Optical properties of thin films of Au@SiO_2 particles', *J. Phys. Chem. B*, 2001, **105**, pp. 3441–3452
64 Yin, Y.D., Lu, Y., Sun, Y.G., and Xia, Y.N.: 'Silver nanowires can be directly coated with amorphous silica to generate well-controlled coaxial nanocables of silver/silica', *Nano Lett.*, 2002, **2**, pp. 427–430
65 Westcott, S.L., Oldenburg, S.J., Lee, T.R., and Halas, N.J.: 'Construction of simple gold nanoparticle aggregates with controlled plasmon-plasmon interactions', *Chem. Phys. Lett.*, 1999, **300**, pp. 651–655
66 Jackson, J.B., and Halas, N.J.: 'Silver nanoshells: Variations in morphologies and optical properties', *J. Phys. Chem. B*, 2001, **105**, pp. 2743–2746
67 Kobayashi, Y., Salgueirino-Maceira, V., and Liz-Marzan, L.M.: 'Deposition of sliver nanoparticles on silica spheres by pretreatment steps in electroless plating', *Chem. Mater.*, 2001, **13**, pp. 1630–1633
68 Averitt, R.D., Sarkar, D., and Halas, N.J.: 'Plasmon resonance shifts of Au-coated Au_2S nanoshells: Insight into multicomponent nanoparticle growth', *Phys. Rev. Lett.*, 1997, **78**, pp. 4217–4220
69 West, J.L., Halas, N., and Sershen, S.R.: 'Optically-responsive nanoshell composites', *Abs. Papers Am. Chem. Soc.*, 2003, **225**, pp. U522–U522
70 Gunnarsson, L., Bjerneld, E.J., Xu, H., Petronis, S., Kasemo, B., and Kall, M.: 'Interparticle Coupling Effects in Nanofabricated Substrates for Surface-Enhanced Raman Scattering', *Appl. Phys. Lett.*, 2001, **78**, pp. 802–804
71 Jensen, T.R., Schatz, G.C., and Van Duyne, R.P.: 'Nanosphere Lithography: Surface plasmon resonance spectrum of a periodic array of silver nanoparticles by UV-vis extinction spectroscopy and electrodynamic modeling', *J. Phys. Chem. B*, 1999, **103**, pp. 2394–2401
72 Felidj, N., Aubard, J., Levi, G., Krenn, J.R., Salerno, M., Schider, G., Lamprecht, B., Leitner, A., and Aussenegg, F.R.: 'Controlling the optical response of regular arrays of gold particles for surface-enhanced Raman scattering', *Phys. Rev. B Condens. Matter Mater. Phys.*, 2002, **65**, pp. 075419/1–075419/9
73 Hulteen, J.C., and Van Duyne, R.P.: 'Nanosphere Lithography: A Materials General Fabrication Process for Periodic Particle Array Surfaces', *J. Vac. Sci. Technol. A, Vac. Surf. Films*, 1995, **13**, pp. 1553–1558
74 Dimitrov, A.S., and Nagayama, K.: 'Continuous convective assembling of fine particles into two-dimensional arrays on solid surfaces', *Langmuir*, 1996, **12**, pp. 1303–1311
75 Dimitrov, A.S., Miwa, T., and Nagayama, K.: 'A comparison between the optical properties of amorphous and crystalline monolayers of silica particles', *Langmuir*, 1999, **15**, pp. 5257–5264
76 Taton, T.A., Lu, G., and Mirkin, C.A.: 'Two-Color Labeling of Oligonucleotide Arrays via Size-Selective Scattering of Nanoparticle Probes', *J. Am. Chem. Soc.*, 2001, **123**, pp. 5164–5165
77 Taton, T.A., Mirkin, C.A., and Letsinger, R.L.: 'Scanometric DNA array detection with nanoparticle probes', *Science*, 2000, **289**, pp. 1757–1760
78 Sonnichsen, C., Geier, S., Hecker, N.E., von Plessen, G., Feldmann, J., Ditlbacher, H., Lamprecht, B., Krenn, J.R., Aussenegg, F.R., Chan, V.Z.-H., Spatz, J.P., and Moller, M.: 'Spectroscopy of single metallic nanoparticles using total internal reflection microscopy', *Appl. Phys. Lett.*, 2000, **77**, pp. 2949–2951
79 Sonnichsen, C., Franzl, T., Wilk, T., von Plessen, G., Feldmann, J., Wilson, O., and Mulvaney, P.: 'Drastic reduction of plasmon damping in gold nanorods', *Phys. Rev. Lett.*, 2002, **88**, pp. 0774021–0774024
80 Bao, P., Frutos, A.G., Greef, C., Lahiri, J., Muller, U., Peterson, T.C., Wardern, L., and Xie, X.: 'High-sensitivity detection of DNA hybridization on microarrays using resonance light scattering', *Anal. Chem.*, 2002, **74**, pp. 1792–1797
81 McFarland, A.D., and Van Duyne, R.P.: 'Single Silver Nanoparticles as Real-Time Optical Sensors with Zeptomole Sensitivity', *Nano Lett.*, 2003, **3**, pp. 1057–1062
82 Van Duyne, R.P., Haes, A.J., and McFarland, A.D.: 'Nanoparticle Optics: Sensing with Nanoparticle Arrays and Single Nanoparticles', *Proc. SPIE-Int. Soc. Opt. Eng.*, 2003, **5223**, pp. 197–207
83 Connolly, S., Cobbe, S., and Fitzmaurice, D.: 'Effects of ligand-receptor geometry and stoichiometry on protein-induced aggregation of biotin-modified colloidal gold', *J. Phys. Chem. B*, 2001, **105**, pp. 2222–2226
84 Malinsky, M.D., Kelly, K.L., Schatz, G.C., and Van Duyne, R.P.: 'Chain Length Dependence and Sensing Capabilities of the Localized Surface Plasmon Resonance of Silver Nanoparticles Chemically Modified with Alkanethiol Self-Assembled Monolayers', *J. Am. Chem. Soc.*, 2001, **123**, pp. 1471–1482
85 Hilger, A., Cuppers, N., Tenfelde, M., and Kreibig, U.: 'Surface and interface effects in the optical properties of silver nanoparticles', *Eur. Phys. J. D*, 2000, **10**, pp. 115–118
86 Henglein, A., and Meisel, D.: 'Spectrophotometric Observations of the Adsorption of Organosulfur Compounds on Colloidal Silver Nanoparticles', *J. Phys. Chem. B*, 1998, **102**, pp. 8364–8366
87 Linnert, T., Mulvaney, P., and Henglein, A.: 'Surface chemistry of colloidal silver: surface plasmon damping by chemisorbed iodide, hydrosulfide (SH-), and phenylthiolate', *J. Phys. Chem.*, 1993, **97**, pp. 679–682
88 Kreibig, U., Gartz, M., and Hilger, A.: 'Mie resonances. Sensors for physical and chemical cluster interface properties', *Ber. Bunsen-Ges.*, 1997, **101**, pp. 1593–1604
89 Nath, N., and Chilkoti, A.: 'A colorimetric gold nanoparticle sensor to interrogate biomolecular interactions in real time on a surface', *Anal. Chem.*, 2002, **74**, pp. 504–509
90 Eck, D., Helm, C.A., Wagner, N.J., and Vaynberg, K.A.: 'Plasmon Resonance Measurements of the Adsorption and Adsorption Kinetics of a Biopolymer onto Gold Nanocolloids', *Langmuir*, 2001, **17**, pp. 957–960
91 Okamoto, T., Yamaguchi, I., and Kobayashi, T.: 'Local plasmon sensor with gold colloid monolayers deposited upon glass substrates', *Opt. Lett.*, 2000, **25**, pp. 372–374
92 Himmelhaus, M., and Takei, H.: 'Cap-shaped gold nanoparticles for an optical biosensor', *Sens. Actuators B, Chem.*, 2000, **B63**, pp. 24–30

93 Takei, H.: 'Biological sensor based on localized surface plasmon associated with surface-bound Au/polystyrene composite microparticles', *Proc. SPIE-Int. Soc. Opt. Eng.*, 1998, **3515**, pp. 278–283
94 Singer, J.M., and Plotz, C.M.: 'The latex fixation test. I. Application to the serologic diagnosis of rheumatoid arthritis', *Am. J. Med.*, 1956, **21**, pp. 888–896
95 Elghanian, R., Storhoff, J.J., Mucic, R.C., Letsinger, R.L., and Mirkin, C.A.: 'Selective colorimetric detection of polynucleotides based on the distance-dependent optical properties of gold nanoparticles', *Science*, 1997, **227**, pp. 1078–1080
96 Mirkin, C.A., Letsinger, R.L., Mucic, R.C., and Storhoff, J.J.: 'A DNA-based method for rationally assembling nanoparticles into macroscopic materials', *Nature*, 1996, **382**, pp. 607–609
97 Mock, J.J., Smith, D.R., and Schultz, S.: 'Local Refractive Index Dependence of Plasmon Resonance Spectra from Individual Nanoparticles', *Nano Lett.*, 2003, **3**, pp. 485–491
98 Mock, J.J., Oldenburg, S.J., Smith, D.R., Schultz, D.A., and Schultz, S.: 'Composite Plasmon Resonant Nanowires', *Nano Lett.*, 2002, **2**, pp. 465–469
99 Stuart, D.A., Haes, A.J., McFarland, A.D., Nie, S. and Van Duyne, R.P. 'Refractive index sensitive, plasmon resonant scattering, and surface enhanced Raman scattering nanoparticles and arrays as biological sensing platforms,' Proc. SPIE, Int. Soc. Opt. Eng., **5327**, 2004, pp. 60–73
100 Nicewarner-Pena, S.R., Griffith Freeman, R., Reiss, B.D., He, L., Pena, D.J., Walton, I.D., Cromer, R., Keating, C.D., and Natan, M.J.: 'Submicrometer metallic barcodes', *Science*, 2001, **294**, pp. 137–141
101 Siiman, O., and Burshteyn, A.: 'Preparation, Microscopy, and Flow Cytometry with Excitation into Surface Plasmon Resonance Bands of Gold or Silver Nanoparticles on Aminodextran-Coated Polystyrene Beads', *J. Phys. Chem. B*, 2000, **104**, pp. 9795–9810
102 Turner, A.P.F.: 'Biosensors—Sense and Sensitivity', *Science*, 2000, **290**, pp. 1315–1317
103 Klotz, I.M.: 'Ligand-Receptor Energetics: A Guide for the Perplexed', (Wiley, New York, N.Y., 1997)
104 Lee, H.J., Goodrich, T.T., and Corn, R.M.: 'SPR imaging measurements of 1-D and 2-D DNA microarrays created from microfluidic channels on gold thin films', *Anal. Chem.*, 2001, **73**, pp. 5525–5531
105 Hall, D.: 'Use of optical biosensors for the study of mechanistically concerted surface adsorption processes', *Anal. Biochem.*, 2001, **288**, pp. 109–125
106 Wang, J., Cai, X., Rivas, G., Shiraishi, H., Farias, P.A.M., and Dontha, N.: 'DNA Electrochemical Biosensor for the Detection of Short DNA Sequences Related to the Human Immunodeficiency Virus', *Anal. Chem.*, 1996, **68**, pp. 2629–2634
107 Walterbeek, H.T., and van der Meer, A.J.G.M.: 'A sensitive and quantitative biosensing method for the determination of γ-ray emitting radionuclides in surface water', *J. Environ. Radioact.*, 1996, **33**, pp. 237–254
108 Thevenot, D.R., Toth, K., Durst, R.A., and Wilson, G.S.: 'Electrochemical biosensors: recommended definitions and classification', *Biosens. Bioelectron.*, 2001, **16**, pp. 121–131
109 Mascini, M., Palchetti, I., and Marrazza, G.: 'DNA electrochemical biosensors', *Fresenius J. Anal. Chem.*, 2001, **369**, pp. 15–22
110 Horacek, J., and Skladal, P.: 'Improved direct piezoelectric biosensors operating in liquid solution for the competitive label-free immunoassay of 2,4-dichlorophenoxyacetic acid', *Anal. Chim. Acta*, 1997, **347**, pp. 43–50
111 Ebersole, R.C., Miller, J.A., Moran, J.R., and Ward, M.D.: 'Spontaneously formed functionally active avidin monolayers on metal surfaces: a strategy for immobilizing biological reagents and design of piezoelectric biosensors', *J. Am. Chem. Soc.*, 1990, **112**, pp. 3239–3241
112 Miller, M.M., Sheehan, P.E., Edelstein, R.L., Tamanaha, C.R., Zhong, L., Bounnak, S., Whitman, L.J., and Colton, R.J.: 'A DNA array sensor utilizing magnetic microbeads and magnetoelectronic detection', *J. Magn. Magn. Mater.*, 2001, **225**, pp. 156–160
113 Chemla, Y.R., Grossman, H.L., Poon, Y., McDermott, R., Stevens, R., Alper, M.D., and Clarke, J.: 'Ultrasensitive magnetic biosensor for homogeneous immunoassay', *Proc. Natl. Acad. Sci. USA*, 2000, **97**, p. 26
114 Raiteri, R., Grattarola, M., Butt, H.-J., and Skladal, P.: 'Micromechanical cantilever-based biosensors', *Sens. Actuators B, Chem.*, 2001, **79**, pp. 115–126
115 Kasemo, B.: 'Biological surface science', *Curr. Opin. Solid State Mater. Sci.*, 1998, **3**, pp. 451–459
116 Natsume, T., Nakayama, H., and Isobe, T.: 'BIA-MS-MS: biomolecular interaction analysis for functional proteomics', *Trends Biotechnol.*, 2001, **19**, pp. S28–S33
117 Polla, D.L., Erdman, A.G., Robbins, W.P., Markus, D.T., Diaz-Diaz, J., Rizq, R., Nam, Y., Brickner, H.T., Wang, A., and Krulevitch, P.: 'Microdevices in medicine', *Annu. Rev. Biomed. Eng.*, 2000, **2**, pp. 551–576
118 Liedberg, B., Nylander, C., and Lundstroem, I.: 'Surface plasmon resonance for gas detection and biosensing', *Sens. Actuators*, 1983, **4**, pp. 299–304
119 Reather, H.: 'Surface Polaritons on Smooth and Rough Surfaces and on Gratings' (Springer-Verlag, Berlin, 1988)
120 Jung, L.S., Campbell, C.T., Chinowsky, T.M., Mar, M.N., and Yee, S.S.: 'Quantitative Interpretation of the Response of Surface Plasmon Resonance Sensors to Adsorbed Films', *Langmuir*, 1998, **14**, pp. 5636–5648
121 Jung, L.S., and Campbell, C.T.: 'Sticking Probabilities in Adsorption of Alkanethiols from Liquid Ethanol Solution onto Gold', *J. Phys. Chem. B*, 2000, **104**, pp. 11168–11178
122 Jung, L.S., and Campbell, C.T.: 'Sticking Probabilities in Adsorption from Liquid Solutions: Alkylthiols on Gold', *Phys. Rev. Lett.*, 2000, **84**, pp. 5164–5167
123 Jung, L.S., Nelson, K.E., Stayton, P.S., and Campbell, C.T.: 'Binding and Dissociation Kinetics of Wild-Type and Mutant Streptavidins on Mixed Biotin-Containing Alkylthiolate Monolayers', *Langmuir*, 2000, **16**, pp. 9421–9432
124 Perez-Luna, V.H., O'Brien, M.J., Opperman, K.A., Hampton, P.D., Lopez, G.P., Klumb, L. A., and Stayton, P.S.: 'Molecular Recognition between Genetically Engineered Streptavidin and Surface-Bound Biotin', *J. Am. Chem. Soc.*, 1999, **121**, pp. 6469–6478
125 Mann, D.A., Kanai, M., Maly, D.J., and Kiessling, L.L.: 'Probing Low Affinity and Multivalent Interactions with Surface Plasmon Resonance: Ligands for Concanavalin A', *J. Am. Chem. Soc.*, 1998, **120**, pp. 10575–10582
126 Hendrix, M., Priestley, E.S., Joyce, G.F., and Wong, C.-H.: 'Direct Observation of Aminoglycoside-RNA Interactions by Surface Plasmon Resonance', *J. Am. Chem. Soc.*, 1997, **119**, pp. 3641–3648
127 Frey, B.L., Jordan, C.E., Kornguth, S., and Corn, R.M.: 'Control of the Specific Adsorption of Proteins onto Gold Surfaces with Poly(L-lysine) Monolayers', *Anal. Chem.*, 1995, **67**, pp. 4482–4457
128 Mrksick, M., Grunwell, J.R., and Whitesides, G.M.: 'Biospecific Adsorption of Carbonic Anhydrase to Self-Assembled Monolayers of Alkanethiolates That Present Benzenesulfonamide Groups on Gold', *J. Am. Chem. Soc.*, 1995, **117**, pp. 12009–12010
129 Rao, J., Yan, L., Xu, B., and Whitesides, G.M.: 'Using surface plasmon resonance to study the binding of vancomycin and its dimer to self-assembled monolayers presenting D-Ala-D-Ala', *J. Am. Chem. Soc.*, 1999, **121**, pp. 2629–2630
130 Berger, C.E.H., Beumer, T.A.M., Kooyman, R.P.H., and Greve, J.: 'Surface Plasmon Resonance Multisensing', *Anal. Chem.*, 1998, **70**, pp. 703–706
131 Heaton, R.J., Peterson, A.W., and Georgiadis, R.M.: 'Electrostatic surface plasmon resonance: direct electric field-induced hybridization and denaturation in monolayer nucleic acid films and label-free discrimination of base mismatches', *Proc. Natl. Acad. Sci. USA*, 2001, **98**, pp. 3701–3704
132 Georgiadis, R., Peterlinz, K.P., and Peterson, A.W.: 'Quantitative Measurements and Modeling of Kinetics in Nucleic Acid Monolayer Films Using SPR Spectroscopy', *J. Am. Chem. Soc.*, 2000, **122**, pp. 7837–3173
133 Jordan, C.E., Frutos, A.G., Thiel, A.J., and Corn, R.M.: 'Surface plasmon resonance imaging measurements of DNA hybridization adsorption and streptavidin/DNA multilayer formation at chemically modified gold surfaces', *Anal. Chem.*, 1997, **69**, pp. 4939–4947
134 Nelson, B.P., Grimsrud, T.E., Liles, M.R., and Goodman, R.M.: 'Surface Plasmon Resonance Imaging Measurements of DNA and RNA Hybridization Adsorption onto DNA Microarrays', *Anal. Chem.*, 2001, **73**, pp. 1–7
135 Brockman, J.M., Frutos, A.G., and Corn, R.M.: 'A Multistep Chemical Modification Procedure To Create DNA Arrays on Gold Surfaces for the Study of Protein-DNA Interactions with Surface Plasmon Resonance Imaging', *J. Am. Chem. Soc.*, 1999, **121**, pp. 8044–8051
136 Haake, H.-M., Schutz, A., and Gauglitz, G.: 'Label-free detection of biomolecular interaction by optical sensors', *Fresenius J. Anal. Chem.*, 2000, **366**, pp. 576–585
137 Brockman, J.M., Nelson, B.P., and Corn, R.M.: 'Surface Plasmon Resonance Imaging Measurements of Ultrathin Organic Films', *Annu. Rev. Phys. Chem.*, 2000, **51**, pp. 41–63
138 Shumaker-Parry, J.S., Zareie, M.H., Aebersold, R., and Campbell, C.T.: 'Microspotting Streptavidin and Double-Stranded DNA Arrays on Gold for High-Throughput Studies of Protein-DNA Interactions by Surface Plasmon Resonance Microscopy', *Anal. Chem.*, 2004, **76**, pp. 918–929
139 Schuck, P.: 'Use of Surface Plasmon Resonance to Probe the Equilibrium and Dynamic Aspects of Interactions between Bilogical Macromolecules', *Ann. Rev. Biophys. Biomol. Struct.*, 1997, **26**, pp. 541–566
140 Garland, P.B.: 'Optical evanescent wave methods for the study of biomolecular interactions', *Q. Rev. Biophys.*, 1996, **29**, pp. 91–117
141 Knoll, W.: 'Interfaces and thin films as seen by bound electromagnetic waves', *Annu. Rev. Phys. Chem.*, 1998, **49**, pp. 569–638
142 Shumaker-Parry, J.S., and Campbell, C.T.: 'Quantitative Methods for Spatially Resolved Adsorption/Desorption Measurements in Real Time by Surface Plasmon Resonance Microscopy', *Anal. Chem.*, 2004, **76**, pp. 907–917
143 Karlsson, R., and Stahlberg, R.: 'Surface Plasmon Resonance detection and multispot sensing for direct monitoring of interactions involving low-molecular weight analytes and for determination of low affinities', *Anal. Biochem.*, 1995, **228**, pp. 274–280
144 Sjolander, S., and Urbaniczky, C.: 'Integrated fluid handling-system for biomolecular interaction analysis', *Anal. Chem.*, 1991, **63**, pp. 2338–2345
145 Yonzon, C.R., Zou, S., Jeoung, E., Schatz, G.C., Mrksich, M., Van Duyne, R.P. 'A Comparative Analysis of Localized and Propagating Surface Plasmon Resonance Sensors: The Binding of Concanavalin

A to a Monosaccharide Functionalized Self-Assembled Monolayer,' J. Am. Chem. Soc., 2004, **126**, pp. 12667–12676
146 Hardman, K.D., and Ainsworth, C.F.: 'Structure of concanavalin A at 2.4-Ang resolution', *Biochemistry*, 1972, **11**, pp. 4910–4919
147 Smith, E.A., Thomas, W.D., Kiessling, L.L., and Corn, R.M.: 'Surface Plasmon Resonance Imaging Studies of Protein-Carbohydrate Interactions', *J. Am. Chem. Soc.*, 2003, **125**, pp. 6140–6148
148 Lee, Y., Martin, C.D., Parise, J.B., Hriljac, J.A., and Vogt, T.: 'Formation and manipulation of confined water wires', *Nano Lett.*, 2004, **4**, pp. 619–621
149 Alzheimer, A., Stelzmann, R.A., Schnitzlein, H.N., and Murtagh, F.R.: 'An English translation of Alzheimer's 1907 paper, "Uber eine eigenartige Erkankung der Hirnrinde"', *Clin Anat*, 1995, **8**, pp. 429–31
150 Hardy, J.A., and Higgins, G.A.: 'Alzheimer's disease: the amyloid cascade hypothesis', *Science*, 1992, **256**, pp. 184–185
151 Klein, W.L., Krafft, G.A., and Finch, C.E.: 'Targeting small A beta oligomers: the solution to an Alzheimer's disease conundrum?', *Trends Neurosci.*, 2001, **24**, pp. 219–224
152 Lorenzo, A., and Yankner, B.A.: 'Beta-amyloid neurotoxicity requires fibril formation and is inhibited by congo red', *Proc. Natl. Acad. Sci. USA*, 1994, **91**, pp. 12243–12247
153 Lambert, M.P., Barlow, A.K., Chromy, B.A., Edwards, C., Freed, R., Liosatos, M., Morgan, T.E., Rozovsky, I., Trommer, B., Viola, K.L., Wals, P., Zhang, C., Finch, C.E., Krafft, G.A., and Klein, W.L.: 'Diffusible, nonfibrillar ligands derived from A beta(1-42) are potent central nervous system neurotoxins', *Proc. Natl. Acad. Sci. USA*, 1998, **95**, pp. 6448–6453
154 Gong, Y., Chang, L., Viola, K.L., Lacor, P.N., Lambert, M.P., Finch, C.E., Krafft, G.A., and Klein, W.L.: 'Alzheimer's disease-affected brain: Presence of oligomeric Ab ligands (ADDLs) suggests a molecular basis for reversible memory loss', *Proc. Natl. Acad. Sci. USA*, 2003, **100**, pp. 10417–10422
155 Haes, A.J., Chang, L., Klein, W.L., Van Duyne, R.P., and Hall, W.P.: 'First Steps Toward an Alzheimer's Disease Assay using Localized Surface Plasmon Resonance Spectroscopy', *Northwestern University Invention Disclosure*, 2004, 24017
156 Haes, A.J., Hall, W.P., Chang, L., Klein, W.L., and Van Duyne, R.P.: 'A localized surface plasmon resonance biosensor: First steps toward an assay for Alzheimer's disease', *Nano Lett.*, 2004, **4**, pp. 1029–1034
157 Klar, T., Perner, M., Grosse, S., von Plessen, G., Spirkl, W., and Feldmann, J.: 'Surface-Plasmon Resonances in Single Metallic Nanoparticles', *Phys. Rev. Lett.*, 1998, **80**, pp. 4249–4252
158 Raschke, G., Kowarik, S., Franzl, T., Sonnichsen, C., Klar, T.A., and Feldmann, J.: 'Biomolecular Recognition Based on Single Gold Nanoparticle Light Scattering', *Nano Lett.*, 2003, **3**, pp. 935–938
159 Malinsky, M.D., Kelly, K.L., Schatz, G.C., and Van Duyne, R.P.: 'Nanosphere Lithography: Effect of Substrate on the Localized Surface Plasmon Resonance Spectrum of Silver Nanoparticles', *J. Phys. Chem. B*, 2001, **105**, pp. 2343–2350
160 Draine, B.T., and Flatau, P.J.: 'Discrete-dipole approximation for scattering calculations', *J. Opt. Soc. Am. A, Opt Image Sci. Vis.*, 1994, **11**, pp. 1491–1499
161 Kelly, K.L., Coronado, E., Zhao, L., and Schatz, G.C.: 'The Optical Properties of Metal Nanoparticles: The Influence of Size, Shape, and Dielectric Environment', *J. Phys. Chem. B*, 2003, **107**, pp. 668–677
162 Lynch, D.W., and Hunter, W.R.: *in* Palik, E.D. (ed.): 'Handbook of Optical Constants of Solids' (Academic Press, New York, 1985), pp. 350–356
163 Jensen, T.R., Kelly, K.L., Lazarides, A., and Schatz, G.C.: 'Electrodynamics of noble metal nanoparticles and nanoparticle clusters', *J. Cluster Sci.*, 1999, **10**, pp. 295–317
164 Raman, C.V., and Krishnan, K.S.: *Nature*, 1928, **121**, p. 501
165 McCreery, R.L.: 'Raman Spectroscopy for Chemical Analysis', 1st Edn. (John Wiley & Sons, Inc., New York, , 2000), Vol. 157
166 Cotton, T.M., Kim, J.H., and Chumanov, G.D.: 'Application of Surface-Enhanced Raman-Spectroscopy to Biological-Systems', *J. Raman Spectrosc.*, 1991, **22**, pp. 729–742
167 Nabiev, I., Chourpa, I., and Manfait, M.: 'Applications of Raman and Surface-Enhanced Raman-Scattering Spectroscopy in Medicine', *J. Raman Spectrosc.*, 1994, **25**, pp. 13–23
168 Petry, R., Schmitt, M., and Popp, J.: 'Raman Spectroscopy - A prospective tool in the life sciences', *Chemphyschem*, 2003, **4**, pp. 14–30
169 Campion, A., and Kambhampati, P.: 'Surface-enhanced Raman scattering', , 1998, **27**, pp. 241–250
170 Otto, A.: 'Surface-Enhanced Raman-Scattering of Adsorbates', 1991, **22**, pp. 743–752
171 Jeanmaire, D.L., and Van Duyne, R.P.: 'Surface Raman spectroelectrochemistry. Part I. Heterocyclic, aromatic, and aliphatic amines adsorbed on the anodized silver electrode', *J. Electroanal. Chem. Interfacial Electrochem.*, 1977, **84**, pp. 1–20
172 Campion, A., and Kambhampati, P.: 'Surface-enhanced Raman scattering', *Chem. Soc. Rev.*, 1998, **27**, pp. 241–250
173 Otto, A., Bruckbauer, A., and Chen, Y.X.: 'On the chloride activation in SERS and single molecule SERS', *J. Mol. Struct.*, 2003, **661**, pp. 501–514
174 Hildebrandt, P., and Stockburger, M.: 'Surface-Enhanced Resonance Raman-Spectroscopy of Rhodamine-6 g Adsorbed on Colloidal Silver', *J. Phys. Chem.*, 1984, **88**, pp. 5935–5944
175 Doering, W.E., and Nie, S.M.: 'Single-molecule and single-nanoparticle SERS: Examining the roles of surface active sites and chemical enhancement', *J. Phys. Chem. B*, 2002, **106**, pp. 311–317
176 Otto, A.: 'On the electronic contribution to single molecule surface enhanced Raman spectroscopy', *Indian J. Phys. B*, 2003, **77B**, pp. 63–73
177 Nie, S.M., and Emory, S.R.: 'Probing single molecules and single nanoparticles by surface-enhanced Raman scattering', *Science*, 1997, **275**, pp. 1102–1106
178 Kneipp, K., Wang, Y., Kneipp, H., Perelman, L.T., Itzkan, I., Dasari, R., and Feld, M.S.: 'Single molecule detection using surface-enhanced Raman scattering (SERS)', *Phys. Rev. Lett.*, 1997, **78**, pp. 1667–1670
179 Moskovits, M.: 'Enhanced Raman-Scattering by Molecules Adsorbed on Electrodes - Theoretical-Model', *Solid State Commun.*, 1979, **32**, pp. 59–62
180 Kennedy, B.J., Spaeth, S., Dickey, M., and Carron, K.T.: 'Determination of the Distance Dependence and Experimental Effects for Modified SERS Substrates Based on Self-Assembled Monolayers Formed Using Alkanethiols', *J. Phys. Chem. B*, 1999, **103**, pp. 3640–3646
181 Ye, Q., Fang, J.X., and Sun, L.: 'Surface-enhanced Raman scattering from functionalized self-assembled monolayers .2. Distance dependence of enhanced Raman scattering from an azobenzene terminal group', 1997, **101**, pp. 8221–8224
182 Tsen, M., and Sun, L.: 'Surface-Enhanced Raman-Scattering from Functionalized Self-Assembled Monolayers .1. Distance Dependence of Enhanced Raman-Scattering from a Terminal Phenyl Group', , 1995, **307**, pp. 333–340
183 Keating, C.D., Kovaleski, K.M., and Natan, M.J.: 'Protein : colloid conjugates for surface enhanced Raman scattering: Stability and control of protein orientation', *J. Phys. Chem. B*, 1998, **102**, pp. 9404–9413
184 Keating, C.D., Kovaleski, K.K., and Natan, M.J.: 'Heightened electromagnetic fields between metal nanoparticles: Surface enhanced Raman scattering from metal-cytochrome c-metal sandwiches', *J. Phys. Chem. B*, 1998, **102**, pp. 9414–9425
185 Billman, J., and Otto, A.: 'Charge-Transfer between Adsorbed Cyanide and Silver Probed by SERS', *Surf. Sci.*, 1984, **138**, pp. 1–25
186 Farquharson, S., Gift, A.D., Maksymiuk, P., and Inscore, F.E.: 'Rapid dipicolinic acid extraction from bacillus spores detected by surface-enhanced Raman spectroscopy', *Appl. Spectrosc.*, 2004, **58**, pp. 351–354
187 Zhang, X., Yonzon, C.R., and Van Duyne, R.P.: 'An electrochemical surface-enhanced Raman spectroscopy approach to anthrax detection', *Proc. SPIE- Int. Soc. Opt. Eng.*, 2003, **5221**, pp. 82–91
188 Mulvaney, S.P., and Keating, C.D.: 'Raman spectroscopy', *Anal. Chem.*, 2000, **72**, pp. 145R–157R
189 Schrader, B., Dippel, B., Erb, I., Keller, S., Lochte, T., Schulz, H., Tatsch, E., and Wessel, S.: 'NIR Raman spectroscopy in medicine and biology: results and aspects', *J. Mol. Struct.*, 1999, **481**, pp. 21–32
190 Carey, P.R.: 'Raman spectroscopy, the sleeping giant in structural biology, awakes', *J. Biol. Chem.*, 1999, **274**, pp. 26625–26628
191 Lyon, L.A., Keating, C.D., Fox, A.P., Baker, B.E., He, L., Nicewarner, S.R., Mulvaney, S.P., and Natan, M.J.: 'Raman spectroscopy', *Anal. Chem.*, 1998, **70**, pp. 341R–361R
192 Kneipp, K., Kneipp, H., Itzkan, I., Dasari, R.R., and Feld, M.S.: 'Surface-enhanced Raman scattering: A new tool for biomedical spectroscopy', *Curr. Sci.*, 1999, **77**, pp. 915–924
193 Sokolov, K., Aaron, J., Hsu, B., Nida, D., Gillenwater, A., Follen, M., MacAulay, C., Adler-Storthz, K., Korgel, B., Descour, M., Pasqualini, R., Arap, W., Lam, W., and Richards-Kortum, R.: 'Optical systems for in vivo molecular imaging of cancer', *Technol. Cancer Research Treatment*, 2003, **2**, pp. 491–504
194 Carey, P.R.: 'Raman spectroscopy in enzymology: the first 25 years', *J. Raman Spectrosc.*, 1998, **29**, pp. 7–14
195 Ooka, A.A., and Garrell, R.L.: 'Surface-enhanced Raman spectroscopy of DOPA-containing peptides related to adhesive protein of marine mussel, Mytilus edulis', *Biopolymers*, 2000, **57**, pp. 92–102
196 Picorel, R., Chumanov, G., Cotton, T.M., Montoya, G., Toon, S., and Seibert, M.: 'Surface-Enhanced Resonance Raman-Scattering Spectroscopy of Photosystem-Ii Pigment-Protein Complexes', *J. Phys. Chem.*, 1994, **98**, pp. 6017–6022
197 Rivas, L., Murza, A., Sanchez-Cortes, S., and Garcia-Ramos, J.V.: 'Adsorption of acridine drugs on silver: surface-enhanced resonance Raman evidence of the existence of different adsorption sites', *Vib. Spectrosc.*, 2001, **25**, pp. 19–28
198 Shen, H.B., Xia, J.F., Zhang, F., Yang, H.F., and Zhang, Z.R.: 'Surface enhanced Raman scattering (SERS) spectra of AMP and DNA in silver sol', *Spectrosc. Spectral Anal.*, 2001, **21**, pp. 798–800
199 Stanicova, J., Kovalcik, P., Chinsky, L., and Miskovsky, P.: 'Preresonance Raman and surface-enhanced Raman spectroscopy study of the complex of the antiviral and antiParkinsonian drug amantadine with histidine', *Vib. Spectrosc.*, 2001, **25**, pp. 41–51
200 Stewart, S., and Fredericks, P.M.: 'Surface-enhanced Raman spectroscopy of peptides and proteins adsorbed on an electrochemically prepared silver surface', *Spectrochim. Acta A, Mol. Biomol. Spectrosc.*, 1999, **55**, pp. 1615–1640
201 Storey, J., Barber, T., Shelton, B., Wachter, E., Carron, K., and Jiang, Y.: 'Applications of Surface-Enhanced Raman-Scattering (Sers) to Chemical-Detection', *Spectroscopy*, 1995, **10**, pp. 20–25
202 Wang, L.Y., Ji, X.H., Yuan, H., Ma, L., Kong, X.G., Liu, Y.C., Yang, W.S., Bai, Y.B., and Li, T.J.: 'Surface-enhanced Raman

spectroscopic study on the interaction of hepatitis B virus surface antigen and its monoclonal antibody', *Acta Chim. Sin.*, 2002, **60**, pp. 2115–2119
203 Wachter, E.A., Storey, J.M.E., Sharp, S.L., Carron, K.T., and Jiang, Y.: 'Hybrid Substrates for Real-Time SERS-Based Chemical Sensors', *Appl. Spectrosc.*, 1995, **49**, pp. 193–199
204 Xu, Y.M., and Liang, L.: 'Surface-Enhanced Resonance Raman-Scattering of R-Phycoerythrin Adsorbed by Silver Hydrosols', *Appl. Spectrosc.*, 1994, **48**, pp. 1147–1149
205 Ye, B.X., Lin, L., Zhang, W.M., and Zhou, X.Y.: 'A study of hemoglobin at silver colloid By surface enhanced Raman spectroscopy', *Chem. J. Chin. Univ.-Chin.*, 1998, **19**, pp. 1239–1241
206 Zeiri, L., Bronk, B.V., Shabtai, Y., Eichler, J., and Efrima, S.: 'Surface-enhanced Raman Spectroscopy as a tool for probing specific biochemical components in bacteria', *Appl. Spectrosc.*, 2004, **58**, pp. 33–40
207 Dou, X.M., and Ozaki, Y.: 'Surface-enhanced Raman scattering of biological molecules on metal colloids: Basic studies and applications to quantitative assay', *Rev. Anal. Chem.*, 1999, **18**, pp. 285–321
208 Maxwell, D.J., Emory, S.R., and Nie, S.M.: 'Nanostructured thin-film materials with Surface-enhanced optical properties', *Chem. Mater.*, 2001, **13**, pp. 1082–1088
209 Dick, L.A., McFarland, A.D., Haynes, C.L., and Van Duyne, R.P.: 'Metal film over nanosphere (MFON) electrodes for surface-enhanced Raman spectroscopy (SERS): Improvements in surface nanostructure stability and suppression of irreversible loss', *J. Phys. Chem. B*, 2002, **106**, pp. 853–860
210 Kneipp, K., Haka, A.S., Kneipp, H., Badizadegan, K., Yoshizawa, N., Boone, C., Shafer-Peltier, K.E., Motz, J.T., Dasari, R.R., and Feld, M.S.: 'Surface-enhanced Raman Spectroscopy in single living cells using gold nanoparticles', *Appl. Spectrosc.*, 2002, **56**, pp. 150–154
211 Jarvis, R.M., and Goodacre, R.: 'Discrimination of bacteria using surface-enhanced Raman spectroscopy', *Anal. Chem.*, 2004, **76**, pp. 40–47
212 Ahern, A.M., and Garrell, R.L.: 'Protein Metal Interactions in Protein-Colloid Conjugates Probed by Surface-Enhanced Raman-Spectroscopy', *Langmuir*, 1991, **7**, pp. 254–261
213 Grabbe, E.S., and Buck, R.P.: 'Evidence for a Conformational Change with Potential of Adsorbed Anti-Igg Alkaline-Phosphatase Conjugate at the Silver Electrode Interface Using SERS', *J. Electroanal. Chem.*, 1991, **308**, pp. 227–237
214 Dick, L.A., Haes, A.J., and Van Duyne, R.P.: 'Distance and orientation dependence of Heterogeneous electron transfer: A surface-enhanced resonance Raman scattering study of cytochrome c bound to carboxylic acid terminated alkanethiols adsorbed on silver electrodes', *J. Phys. Chem. B*, 2000, **104**, pp. 11752–11762
215 Fabriciova, G., Sanchez-Cortes, S., Garcia-Ramos, J.V., and Miskovsky, P.: 'Surface-enhanced Raman spectroscopy study of the interaction of the antitumoral drug emodin with human serum albumin', *Biopolymers*, 2004, **74**, pp. 125–130
216 Nabiev, I.R., Morjani, H., and Manfait, M.: 'Selective Analysis of Antitumor Drug-Interaction with Living Cancer-Cells as Probed by Surface-Enhanced Raman-Spectroscopy', *Eur. Biophys. J.*, 1991, **19**, pp. 311–316
217 He, L., Natan, M.J., and Keating, C.D.: 'Surface-enhanced Raman scattering: A structure specific detection method for capillary electrophoresis', *Anal. Chem.*, 2000, **72**, pp. 5348–5355
218 Carron, K.T., and Kennedy, B.J.: 'Molecular-Specific Chromatographic Detector Using Modified SERS Substrates', *Anal. Chem.*, 1995, **67**, pp. 3353–3356
219 Kennedy, B.J., Milofsky, R., and Carron, K.T.: 'Development of a cascade flow cell for dynamic aqueous phase detection using modified SERS substrates', *Anal. Chem.*, 1997, **69**, pp. 4708–4715
220 Kneipp, K., Kneipp, H., Kartha, V.B., Manoharan, R., Deinum, G., Itzkan, I., Dasari, R.R., and Feld, M.S.: 'Detection and identification of a single DNA base molecule using surface-enhanced Raman scattering (SERS)', *Phys. Rev. E stat. Nonlinear Soft Matter Phys.*, 1998, **57**, pp. R6281–R6284
221 Kneipp, K., Pohle, W., and Fabian, H.: 'Surface Enhanced Raman-Spectroscopy on Nucleic-Acids and Related-Compounds Adsorbed on Colloidal Silver Particles', *J. Mol. Struct.*, 1991, **244**, pp. 183–192
222 Kneipp, K., and Flemming, J.: 'Surface Enhanced Raman-Scattering (SERs) of Nucleic-Acids Adsorbed on Colloidal Silver Particles', *J. Mol. Struct.*, 1986, **145**, pp. 173–179
223 Keller, R.A., Ambrose, W.P., Arias, A.A., Gai, H., Emory, S.R., Goodwin, P.M., and Jett, J.H.: 'Analytical applications of single-molecule detection', *Anal. Chem.*, 2002, **74**, pp. 316a–324a
224 Emory, S.R., and Keller, R.A.: 'Towards efficient and identification of single biomolecules by surface-enhanced Raman scattering', *Proc. SPIE-Int. Soc. Opt. Eng.*, 2000, **2922**, p. 38
225 Xu, H.X., Bjerneld, E.J., Kall, M., and Borjesson, L.: 'Spectroscopy of single hemoglobin molecules by surface enhanced Raman scattering', *Phys. Rev. Lett.*, 1999, **83**, pp. 4357–4360
226 Xu, H.X., Aizpurua, J., Kall, M., and Apell, P.: 'Electromagnetic contributions to single-molecule sensitivity in surface-enhanced Raman scattering', *Phys. Rev. E, Stat. Nonlinear Soft Matter Phys.*, 2000, **62**, pp. 4318–4324
227 Bjerneld, E.J., Foldes-Papp, Z., Kall, M., and Rigler, R.: 'Single-molecule surface-enhanced Raman and fluorescence correlation spectroscopy of horseradish peroxidase', *J. Phys. Chem. B*, 2002, **106**, pp. 1213–1218
228 Bizzarri, A.R., and Cannistraro, S.: 'Surface-enhanced resonance Raman spectroscopy signals from single myoglobin molecules', *Appl. Spectrosc.*, 2002, **56**, pp. 1531–1537
229 Habuchi, S., Cotlet, M., Gronheid, R., Dirix, G., Michiels, J., Vanderleyden, J., De Schryver, F.C., and Hofkens, J.: 'Single-molecule surface enhanced resonance Raman spectroscopy of the enhanced green fluorescent protein', *J. Am. Chem. Soc.*, 2003, **125**, pp. 8446–8447
230 Carey, P.R.: 'Resonance Raman labels and Raman labels', *J. Raman Spectrosc.*, 1998, **29**, pp. 861–868
231 Docherty, F.T., Clark, M., McNay, G., Graham, D., and Smith, W.E.: 'Multiple labelled nanoparticles for bio detection', *Faraday Discuss.*, 2004, **126**, pp. 281–288
232 Dou, X., Takama, T., Yamaguchi, Y., Yamamoto, H., and Ozaki, Y.: 'Enzyme immunoassay utilizing surface-enhanced Raman scattering of the enzyme reaction product', *Anal. Chem.*, 1997, **69**, pp. 1492–1495
233 Vodinh, T., Houck, K., and Stokes, D.L.: 'Surface-Enhanced Raman Gene Probes', *Anal. Chem.*, 1994, **66**, pp. 3379–3383
234 Vo-Dinh, T., Allain, L.R., and Stokes, D.L.: 'Cancer gene detection using surface-enhanced Raman scattering (SERS)', *J. Raman Spectrosc.*, 2002, **33**, pp. 511–516
235 Vo-Dinh, T., Stokes, D.L., Griffin, G.D., Volkan, M., Kim, U.J., and Simon, M.I.: 'Surface-enhanced Raman scattering (SERS) method and instrumentation for genomics and biomedical analysis', *J. Raman Spectrosc.*, 1999, **30**, pp. 785–793
236 Graham, D., Mallinder, B.J., and Smith, W.E.: 'Detection and identification of labeled DNA by surface enhanced resonance Raman scattering', *Biopolymers*, 2000, **57**, pp. 85–91
237 Graham, D., Smith, W.E., Linacre, A.M.T., Munro, C.H., Watson, N.D., and White, P.C.: 'Selective detection of deoxyribonucleic acid at ultralow concentrations by SERRS', *Anal. Chem.*, 1997, **69**, pp. 4703–4707
238 Ni, J., Lipert, R.J., Dawson, G.B., and Porter, M.D.: 'Immunoassay readout method using extrinsic Raman labels adsorbed on immunogold colloids', *Anal. Chem.*, 1999, **71**, pp. 4903–4908
239 Pham, T., Jackson, J.B., Halas, N.J., and Lee, T. R.: 'Preparation and characterization of gold nanoshells coated with self-assembled monolayers', *Langmuir*, 2002, **18**, pp. 4915–4920
240 Stuart, D.A.: 'Biomolecular Imaging and Spectroscopy with Metal and Semiconductor Nanoparticles', 'Analytical Chemistry' (Indiana University, Bloomington, 2003), p. 256
241 Mulvaney, S.P., Musick, M.D., Keating, C.D., and Natan, M.J.: 'Glass-coated, analyte-tagged nanoparticles: A new tagging system based on detection with surface-enhanced Raman scattering', *Langmuir*, 2003, **19**, pp. 4784–4790
242 Cao, Y.W.C., Jin, R.C., and Mirkin, C.A.: 'Nanoparticles with Raman spectroscopic fingerprints for DNA and RNA detection', *Science*, 2002, **297**, pp. 1536–1540
243 Cao, Y.C., Jin, R.C., Nam, J.M., Thaxton, C.S., and Mirkin, C.A.: 'Raman dye-labeled nanoparticle probes for proteins', *J. Am. Chem. Soc.*, 2003, **125**, pp. 14676–14677
244 Krug, J.T., Wang, G.D., Emory, S.R., and Nie, S.M.: 'Efficient Raman enhancement and intermittent light emission observed in single gold nanocrystals', *J. Am. Chem. Soc.*, 1999, **121**, pp. 9208–9214
245 Stuart, D.A., Haes, A.J., McFarland, A.D., Nie, S., and Van Duyne, R.P.: 'Refractive Index Sensitive, Plasmon Resonant Scattering, and Surface Enhanced Raman Scattering Nanoparticles and Arrays as Biological Sensing Platforms', *Proc. SPIE-Int. Soc. Opt. Eng.*, 2004, **5327**, pp. 60–73
246 Dansher, G., Hacker, G.W., Grimelius, L., and Norgaard, J.O.R.: 'Autometallographic Silver Amplificatiton of Colloidal Gold', *J. Histochem.*, 1993, **16**, pp. 201–207
247 Freunscht, P., Van Duyne, R.P., and Schneider, S.: 'Surface-enhanced Raman spectroscopy of trans-stilbene adsorbed on platinum- or self-assembled monolayer-modified silver film over nanosphere surfaces', *Chem. Phys. Lett.*, 1997, **281**, pp. 372–378
248 Farquharson, S., and Maksymiuk, P.: 'Simultaneous chemical separation and surface-enhanced Raman spectral detection using silver-doped sol-gels', *Appl. Spectrosc.*, 2003, **57**, pp. 479–482
249 Stokes, D.L., Pal, A., Narayanan, V.A., and Vo-Dinh, T.: 'Evaluation of a chemical vapor dosimeter using polymer-coated SERS substrates', 1999, **399**, pp. 265–274
250 Sulk, R.A., Corcoran, R.C., and Carron, K.T.: 'Surface enhanced Raman scattering detection of amphetamine and methamphetamine by modification with 2-mercaptonicotinic acid', *Appl. Spectrosc.*, 1999, **53**, pp. 954–959
251 Sulk, R., Chan, C., Guicheteau, J., Gomez, C., Heyns, J.B.B., Corcoran, R., and Carron, K.: 'Surface-enhanced Raman assays (SERA): Measurement of bilirubin and salicylate', *J. Raman Spectrosc.*, 1999, **30**, pp. 853–859
252 Carron, K., Peitersen, L., and Lewis, M.: 'Octadecylthiol-Modified Surface-Enhanced Raman-Spectroscopy Substrates—a New Method for the Detection of Aromatic-Compounds', *Environ. Sci. Technol.*, 1992, **26**, pp. 1950–1954
253 Shafer-Peltier, K.E., Haynes, C.L., Glucksberg, M.R., and Van Duyne, R.P.: 'Toward a glucose biosensor based on surface-enhanced Raman scattering', *J. Am. Chem. Soc.*, 2003, **125**, pp. 588–593
254 Yonzon, C.R., Haynes, C.L., Zhang, X.Y., Walsh, J.T., and Van Duyne, R.P.: 'A glucose biosensor based on surface-enhanced Raman scattering: Improved partition layer, temporal stability,

reversibility, and resistance to serum protein interference', *Anal. Chem.*, 2004, **76**, pp. 78–85
255 Beebe, K.R., Pell, R.J., and Seasholtz, M.B.: 'Chemometrics: A Practical Guide' (John Wiley & Sons, Inc., New York, 1998)
256 Clarke, W.L., Cox, D., Gonder-Frederick, L.A., Carter, W., and Pohl, S.L.: 'Evaluating Clinical Accuracy of Systems for Self-Monitoring of Blood Glucose', *Diabetes Care*, 1987, **10**, pp. 622–628

Copyright of IEE Proceedings -- Nanobiotechnology is the property of IEE and its content may not be copied or emailed to multiple sites or posted to a listserv without the copyright holder's express written permission. However, users may print, download, or email articles for individual use.